PARAMETRIC STUDY OF Ni-BASED CATALYST FOR GLYCEROL DRY REFORMING

by

Özge Selçuk

B.S., Chemical Engineering, Yıldız Technical University, 2016

B.S., Metallurgical and Materials Engineering, Yıldız Technical University, 2016

Submitted to the Institute for Graduate Studies in
Science and Engineering in partial fulfillment of
the requirements for the degree of
Master of Science

Graduate Program in Chemical Engineering
Boğaziçi University
2019

PARAMETRIC STUDY OF Ni-BASED CATALYST FOR GLYCEROL DRY REFORMING

APPROVED BY:

Prof. Ahmet Kerim Avcı . . . .
(Thesis Supervisor)

Prof. Ayşe Nilgün Akın . . . .

Prof. Ramazan Yıldırım . . . .

DATE OF APPROVAL: 01.08.2019

ACKNOWLEDGEMENTS

Many individuals contributed to the production of this thesis and I would like to express my gratitude to all of them. Below I mention just a few of these people, but I do not dare attempting to name and offer thanks to each and everyone individually because to do so properly would require an entire book of itself.

First and foremost, I wish to express my sincere gratitude to my supervisor Prof. Ahmet Kerim Avcı for the continuous support of my MSc study, for his patience, motivation, enthusiasm, and immense knowledge. His guidance helped me in all the time of research and writing of this thesis.

I would like to thank my thesis committee, Prof. Ramazan Yıldırım and Prof. Ayşe Nilgün Akın for providing me with their valuable comments, time and effort they have.

I appreciate the kindness of the departmental support staff Yakup Bal, Dilek Kırkoç, Murat Düzgünoğlu, Şükrü Ordu and Belgin Balkan.

I also want to thank Prof. Mesut Akgün and Gamze Dalgıç who guided me during the early years of my university study and opened the doors of academia for me.

I would like to thank all the members of KB-404, the time I spent together with them was joyful but special thanks to Selin Baç Bilgi, Sinan Koç, Mert Özden, Uğurcan Tozar and Nejdet Semih Altınsoy for their endless support during my study.

I would like to thank my friends, Begüm Yağcı, Elif Esvap, Müge Kasım, Özlem Özbek, Feyza Öner, Şafak Kılıç, Dilara Göreke, Seymen İlke Kaykanat, Pınar Elibol, Ayşegül Karakuş, Ezgi Öztürk and Burcu Oral for accepting nothing less than excellence from me but I wish to point out that although Elif Esvap did not include me in acknowledgment of her MSc thesis, I give a place to her. Shame on her! :P

I spent lots of time in the lab during the day and night to write my thesis. This accomplishment would not have been possible without the companionship of Merve Yüce, Selma Başıbüyük, and Atakan Yüksel.

Special thanks to Merve Yüce and Sevde Büşra Bayrak for providing me with unfailing support and continuous encouragement throughout my years of study.

I thank all my friends but especially to Melike Şatıroğlu and Magdalena Heibeck who were always ready to give their support whenever I needed.

I want to thank my parents, Nazmiye and İbrahim, my brothers, Özer and Sezer and sisters-in-law, Canan and Emel for providing me an incredibly supporting environment that has allowed me to explore the world.

Finally, financial support provided by TÜBİTAK 117M163 and BAP 13880 are acknowledged.

ABSTRACT

PARAMETRIC STUDY OF Ni-BASED CATALYST FOR GLYCEROL DRY REFORMING

Increasing energy demand steers energy industry to find new energy sources. Glycerol, which is by-product of biodiesel, is an alternative to meet this demand. Although there are a number of reforming methods, dry reforming has drawn special attention due to consuming CO_2, which is a greenhouse gas. In this study, glycerol dry reforming over Ni/La_2O_3-ZrO_2 catalyst was carried out. In order to understand the effect of support profoundly, Ni/La_2O_3 and Ni/ZrO_2 catalysts were also prepared and molar CO_2/Glycerol feed ratio (CO_2/G), temperature and residence time, were investigated in the range of 700-750°C, CO_2/G = 1-4 and in the residence time range of 0.5-2.5 mg_{cat} min NmL^{-1} over those three catalysts. In addition to parameter examinations, 72 hours on stream stability tests were performed to observe stability performance of catalysts individually. Optimum parameters were determined as 750°C and CO_2/G feed ratio of 2:1. At these conditions, 38.9% CO_2 conversion was achieved over 20 mg (corresponding to 0.5 mg_{cat} min NmL^{-1} residence time) Ni/La_2O_3-ZrO_2. Stability results showed that Ni/La_2O_3-ZrO_2 has superior stability performance with only 10.1% activation loss compared to Ni/ZrO_2, which was deactivated rapidly and CO_2 conversion became zero after 46 hours.

ÖZET

GLİSEROL KURU REFORMLANMASININ Ni TEMELLİ KATALİZÖRLER ÜZERİNDEKİ PARAMETRİK ÇALIŞMASI

Günümüzde artan enerji talebi, enerji endüstrisini yeni kaynaklar bulmaya yönlendirmektedir. Biyodizelin yan ürünü olan gliserol, bu talebi karşılamak için iyi bir alternatiftir. Başka reform yöntemleri olmasına rağmen, sera gazı olan CO_2'i tüketmesi nedeniyle kuru reformlama süreci dikkat çekmektedir. Bu çalışmada, Ni/La_2O_3-ZrO_2 katalizörü üzerinde gliserol kuru reformlama süreci incelenmiştir. Destek malzemesinin etkisini anlamak için Ni/La_2O_3 ve Ni/ZrO_2 katalizörleri de hazırlanmıştır. Molar CO_2/Gliserol besleme oranı (CO_2/G), sıcaklık ve alıkonma süresi olmak üzere üç ayrı parametre; 700-750°C, $CO_2/G = 1$-4 besleme oranı ve 0.5-2.5 mg_{cat} dk NmL^{-1} alıkonma süresi aralığında incelenmiştir. Parametre taramalarına ek olarak, katali- zörlerin kararlılık performansını bireysel olarak gözlemlemek için 72 saatlik dayanım testleri yapılmıştır. Optimum parametreler 750°C ve $CO_2/G = 2$ besleme oranı olarak belirlenmiştir. Bu şartlarda, 0.5 mg_{cat}dk NmL^{-1} etkileşim süresine karşılık gelen 20 mg katalizör üzerinde %38.9 CO_2 dönüşümü sağlanmış, Ni/La_2O_3 -ZrO_2 katalizörü, termodinamik limite ulaşmıştır. Kararlılık sonuçları, Ni/La_2O_3 -ZrO_2'i, % 10.1 aktivasyon kaybıyla üstün dayanıma sahip olduğunu göstermektedir. Ni/ZrO_2 ise Ni/La_2O_3-ZrO_2'ye kıyasla kısa sürede aktifliğini yitirmiş ve CO_2 dönüşümü 46 saat sonunda sıfırlanmıştır.

TABLE OF CONTENTS

LIST OF FIGURES

LIST OF TABLES

LIST OF SYMBOLS

$d_{particle}$	Diameter of particle (mm)
d_{tube}	Diameter of tube (mm)
E_a	Activation energy (kJ mol^{-1})
F	Total volumetric flow rate (NmL min^{-1})
$F_{i,in}$	Molar flow rate of species in feed (mol min^{-1})
$F_{i,out}$	Molar flow rate of species i in the product stream (mol min^{-1})
L_{bed}	Lenth of bed (mm)
r_g	Glycerol consumption rate (mol g^{-1} s^{-1})
S_i	Selectivity of species i
T	Temperature (°C)
V	Volume (μL)
W	Catalyst weight (mg)
x_i	Conversion with respect to reactant i
Y_i	Yield of species i
α	Reaction order with respect to ethanol
β	Reaction order with respect to CO_2
γ	Reaction order with respect to glycerol
ΔH^o	Standard enthalpy of reaction (kJ mol^{-1})
ν_i	Volumetric flow rate of species i (NmL min^{-1})
ϕ	Reaction order with respect to CO_2

LIST OF ACRONYMS/ABBREVIATIONS

BET	Brauner-Emmett-Teller
CGR	CO_2 to glycerol ratio
DRE	Dry reforming of ethanol
EDS	Energy dispersive spectroscopy
EDX	Energy-dispersive X-ray spectroscopy
EtOH	Ethanol
FESEM	Field emission scanning electron microscopy
FTIR	Fourier transform infrared spectroscopy
FTS	Fischer Tropsch Synthesis
G	Glycerol
GC	Gas chromatograph
GHSV	Gas hourly space velocity
HPLC	High performance liquid chromatograph
MFC	Mass flow controller
MW	Molecular weight
PID	Proportional integral derivative
RWGS	Reverse water gas shift
TEM	Transmission electron microscopy
TGA	Thermogravimetric analysis
TPH	Total petroleum hydrocarbon
TPO	Temperature programmed oxidation
WGS	Water-gas shift
XANES	X-ray absorption near edge structure
XPS	X-ray photoelectron spectroscopy
XRD	X-ray diffraction
XRF	X-ray fluorescence

1. INTRODUCTION

Recent technological developments have increased energy demand which is the driving force behind research on new energy sources. Due to the limited availability of fossil fuels and their consumption causing damage on the environment, those studies mainly focus on sustainable and renewable energy technologies. According to global renewable energy consumption data shown in Figure 1.1, biomass is one of the most promising alternatives for the energy industry. However, direct combustion of biomass releases CO_2, which is considered as a drawback of this option. This disadvantage can be eliminated by producing hydrogen through liquid hydrocarbons which are also generated from biomass.

The use of hydrogen as a fuel is increasing rapidly. To meet hydrogen demand, different raw materials and different production methods are used. Steam reforming, partial oxidation, oxidative reforming (also called autothermal reforming) and dry reforming are the techniques which are used for hydrogen production. These methods have been largely studied except for dry reforming, which is quite new compared to the other methods. Since CO_2 is a reactant of dry reforming, it contributes to CO_2 consumption and a CO and H_2 mixture (so-called syngas) is obtained as a product. Although dry reforming of methanol and ethanol have been studied extensively, there are not many studies about glycerol dry reforming in the literature.

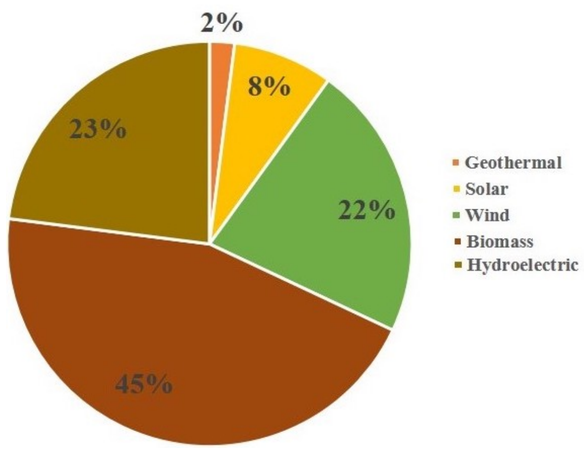

Figure 1.1. Global renewable energy consumption by sources [1].

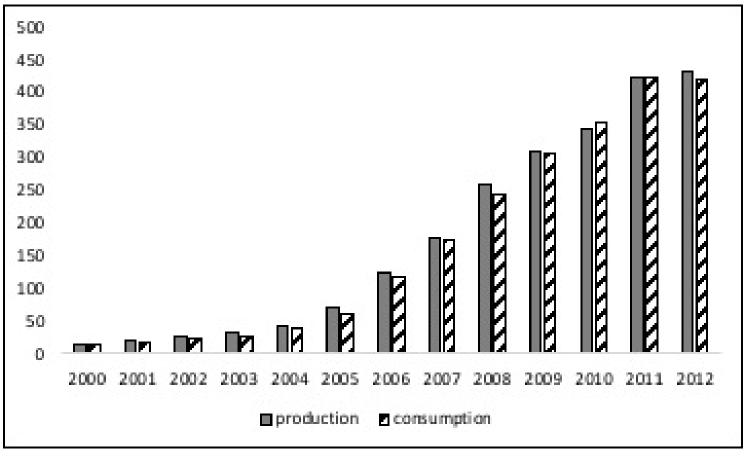

Figure 1.2. Global biodiesel production and consumption by year [1].

Glycerol is a odorless, colorless and viscous solvent, which has 92.1 g mol^{-1} molecular weight and 290°C boiling point [6]. It is a byproduct of biodiesel production whose amount is increased as biodiesel production is increased. Global biodiesel production and consumption data is given in Figure 1.2. As of 2004, production and consumption of biodiesel have a growing trend, which can also be interpreted as an increase on glycerol production. By using glycerol, hydrogen and syngas can be produced alongside with biodiesel. Therefore, biodiesel production can be performed more efficiently. Glycerol dry reforming, a carbon negative way of making syngas, can be described by the following overall reaction:

$$C_3H_8O_3 + CO_2 \rightleftharpoons 4CO + 3H_2 + H_2O \quad \Delta H^0 = 293.2kJmol^{-1} \tag{1.1}$$

As shown in Equation 1.1, reaction of glycerol and CO_2 produces CO, H_2 and water. Since it is an endothermic reaction, external heat supply is necessary to achieve conversion, especially CO_2 conversion. On the other hand, glycerol decomposes at medium temperatures which makes the glycerol dry reforming reaction more complex since side reactions occur. Compared to other reforming reactions, glycerol dry reforming has not been studied in literature extensively. Those studies which focus on glycerol dry reforming mainly have used Ni-based catalysts due to their relatively high activity performance. However, sintering and coke deposition are main drawbacks of

Ni-based catalysts. To overcome these problems, several support materials have been studied in the literature [7–22].

In this study, the glycerol dry reforming reaction has been carried out over Ni-based single and binary oxides supports which are ZrO_2, La_2O_3 and combination of those single oxides namely La_2O_3-ZrO_2. A comprehensive literature survey was carried out in Chapter 2, in which ethanol dry reforming is also included due to the similarity of ethanol and glycerol. In Chapter 3, catalyst preparation, experimental system and system parameters are specified extensively. Thereafter, results of catalytic activity and stability tests are presented comparatively in Results and Discussion (Chapter 4). Lastly, the main findings of this study and recommendations for possible improvements are presented.

2. LITERATURE SURVEY

2.1. Ethanol Dry Reforming

Ethanol is a renewable energy source, which is produced by fermentation of biomass such as sugars, starches or cellulosic materials. Although ethanol is considered as green a energy source, its combustion releases CO_2 to the environment which, hinders it to be a renewable alternative. On the other hand, production of hydrogen from ethanol *via* dry reforming is a good option to create environmentally friendly energy.

$$C_2H_5OH + CO_2 \rightleftharpoons 3CO + 2H_2 \quad \Delta H^0 = 297kJmol^{-1} \tag{2.1}$$

Ethanol dry reforming reaction is intensely endothermic, which means additional heat has to be supplied to the system, and only a CO and H_2 mixture, which is also known as syngas, is obtained as product. Beside this advantage, the negative impact of CO_2, which is byproduct of fermentation reaction can also be compensated by using CO_2 as reactant in dry reforming reaction.

2.1.1. Thermodynamic Analysis

Although there are many studies which performed thermodynamic analysis of dry reforming, the study of Wang and Wang [23] focused on thermodynamic analysis of ethanol dry reforming in detail. Gibbs free energy minimization method was used in this work which was carried out within the CO_2/EtOH ratio range of 0-5 , temperature range of 500-1500 K and pressure range of 0.1-2 MPa. As a result of this study, optimized conditions of ethanol dry reforming were determined between 1200-1300 K temperature and varying CO_2/EtOH ratio between 1.2-1.3 at 0.1 MPa. At these conditions, about 95% H_2 yield and 97% CO yield were obtained. While CH_4, H_2, H_2O, CO, CO_2 and $C_{(s)}$ were observed, other hydrocarbons such as C_2H_4 and C_2H_6 were not seen in products of this thermodynamic study. Furthermore, carbon formation was encountered at optimal conditions.

In the study of Kale and Kulkarni [24], thermodynamic analysis of ethanol autothermal CO_2 reforming was conducted to specify thermoneutral conditions which allows to obtain products other than syngas such as hydrogen and carbon. Results showed that maximum syngas production (2.58 moles) was achieved at 1 bar, 1:1 CO_2/EtOH and 1:2 O_2/EtOH ratio. At these conditions, thermoneutral temperature was determined to be 603.55°C and other than syngas, 0.82, 0.2 and 0.89 mole carbon, methane and water were obtained respectively. Furthermore, it was seen that carbon formation deteriorates with rising pressure. Pressure increase boosts the syngas ratio which is desirable for FTS and CO_2 conversion but affects H_2 production negatively.

Another thermodynamic investigation of ethanol dry reforming was carried out in the entity of reducing agents such as glycine, hydrazine, urea and ammonia by Kumar *et al.* [25]. This study was conducted at the temperature range of 300-1200 K and 1 atm pressure. Due to increased H_2 yield and hindered the coke formation, hydrazine was identified as the best agent among other agents which were used in this study.

2.1.2. Catalysts

In the literature, apart from thermodynamic analysis of ethanol dry reforming, there are also other studies that involve experimental investigations. In these studies, different catalysts are used. Due to its high activity and comparatively low price, Ni has been preferred in most of the studies.

The work of Bellido *et al.* [26] focused on comparison of Ni/Y_3O_3 -ZrO_2 synthesis methods which are wet impregnation and polymerization. Results showed that less NiO agglomeration and more Ni dispersion were observed by polymerization. Later, two different Ni loadings which are 5 and 10 wt.% Ni/Y_3O_3 -ZrO_2 were prepared by polymerization and wet impregnation and loaded into a fixed-bed down-flow quartz reactor in which CO_2 reforming of ethanol was performed. Ethanol flow rate and CO_2/EtOH ratio were fixed to 1.3 mL.h^{-1} and 1:1, respectively. At 800°C, 61% CO_2 conversion with no carbon formation was achieved by 5% loading which synthesized by polymerization method.

As another study, Hu and Lu [27] conducted ethanol dry reforming over Ni/Al_2O_3 catalyst. In their experimental work, working conditions were determined as the temperature range of 500-800°C and 3:1 CO_2/EtOH molar ratio. Together with observing severe coke formation at lower temperatures and CO_2/EtOH ratios, equally comprised syngas composition (1:1 CO/H_2 ratio) was achieved above 700°C.

Zawadzki *et al.* [28] conducted ethanol CO_2 reforming over Ni catalysts which are prepared by using different single supports such as Al_2O_3, CeO_2 , MgO and ZrO_2. Results showed that Ni supported on CeO_2 had better DRE performance, having preferably good H_2 selectivity at 750°C with respect to the one which was performed at 700°C. According to this result, as temperature was increased from 700° to 750°C with high CO_2/EtOH ratios, H_2 production was improved and carbon formation (especially filamentous form) was inhibited.

In the study of Bahari *et al.* [29], Ce-promoted and un-promoted 10%Ni/Al_2O_3 catalysts were prepared and then those catalyst were tested in ethanol dry reforming reaction to determine the effect of Ce as promoter on ethanol conversion. The reaction was performed at two different CO_2/EtOH ratios which are 2.5:1 and 1:2.5, between 923 to 973 K and at 1 atm. Their findings showed that ethanol conversion of 10% Ni/Al_2O_3 was improved to a maximum level of 75.2% by increasing temperature from 923 to 973 K. On the other hand, while stability of the catalyst during 5-7 hour time on stream experiments was not affected by being Ce-promoted or not, Ce promoted catalysts had better catalytic activity as against to the one which was not promoted due to its oxygen mobility which helped to oxidize formatted carbon located on Ni particles. In addition, graphitic and amorphous type carbons were observed in both but promoted catalyst placed at the top of the filamentous carbon whereas unpromoted one was sheathed by multi-walled carbon nanofibers which also contributed the exceptional activity of the Ce-promoted catalyst.

Bahari *et al.* [30, 31] conducted two successive ethanol dry reforming studies in 2016 and 2017. In the former study [30], effect of different La loading range between 0-5% on Ni/Al_2O_3 was investigated. It was seen that 3% La amount as promoter was the best to reach optimum value of ethanol conversion. In the latter [31], ethanol dry reforming over 3%La-promoted Ni/Al_2O_3 catalyst was performed under the following conditions: 20 kPa CO_2 and ethanol partial pressure and in the temperature range of 923-973 K. They found that increasing temperature did not change the catalyst stability and ethanol conversion was observed to reach the highest level of 45.5% at 973 K. Later, to observe the effect of CO_2 partial pressure, it was increased incrementally from 0 to 50 kPa at 973 K while ethanol pressure was fixed to 20 kPa. As a result of this experiment, ethanol conversion was enhanced from 26.3 to 45.5% and H_2 yield was doubled. Lastly, to observe the effect of ethanol partial pressure on ethanol dry reforming, ethanol partial pressure was varied from 10 to 50 kPa at 20 kPa constant CO_2 partial pressure and 973 K. The highest conversion which is about 37% was achieved at 40kPa. The study conducted by Bej *et al.* [32] focused on H_2 production over NiO/Al_2O_3 catalyst with different Ni loading range between 5-15%. It was seen that 10% Ni had superior catalytic activity among others. In the study, optimum operating parameters were also investigated and experiments were carried out in the temperature range of 500-850°C, 0.5-2 CO_2/EtOH feed ratio and 19.0-41.8 kg_{cat} h $kmol^{-1}$ space time. Results showed that optimum operating parameters were determined as 750°C temperature, 1.4 CO_2/EtOH ratio and 24.90 kg_{cat} h $kmol^{-1}$ space time. Under these conditions, 76% CO_2 conversion were obtained.

2.2. Glycerol Dry Reforming

Increasing energy demand directs energy industry to be in quest of new energy sources. Glycerol which is a side product of biodiesel production has been found to be one of these promising alternatives to fulfill this demand. As new sources have been searched, alternative routes have been also investigated. This is because glycerol dry reforming has brought a new and green perspective to the energy sector, utilizing the greenhouse gas CO_2 (as shown in Equation 2.2) and, therefore, drawing a great deal of attention to this method.

$$C_3H_8O_3 + CO_2 \rightleftharpoons 4CO + 3H_2 + H_2O \quad \Delta H^0 = 293.2kJmol^{-1} \tag{2.2}$$

$$C_3H_8O_3 \rightleftharpoons 3CO + 4H_2 \quad \Delta H^0 = 251.2kJmol^{-1} \tag{2.3}$$

$$H_2 + CO_2 \rightleftharpoons CO + H_2O \quad \Delta H^0 = 41.2kJmol^{-1} \tag{2.4}$$

RWGS (Equation 2.4) and glycerol decomposition (Equation 2.3) reactions play an important role in glycerol dry reforming. Due to high temperature and high atomic content of glycerol, its decomposition produces several chemicals viewed in Figure 2.1 by means of side reactions.

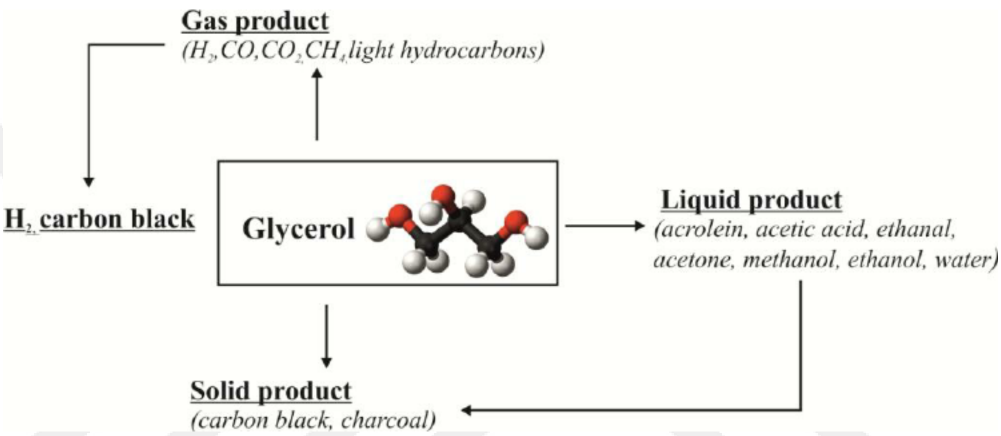

Figure 2.1. Products obtained by glycerol decomposition [2].

One of those reactions is glycerol dehydration (Equation 2.7) which forms acetol and water. Then, acetol decomposes (Equation 2.6) *via* increasing temperature and produces acrolein which also decomposes to hydrogen, carbon monoxide and some hydrocarbons such as ethylene, ethane and propanal.

$$C_3H_8O_3 \rightleftharpoons C_3H_6O_2 + H_2O \quad \Delta H^0 = 450kJmol^{-1} \tag{2.5}$$

$$C_3H_6O_2 \rightleftharpoons C_3H_4O + H_2O \quad \Delta H^0 = -36kJmol^{-1} \tag{2.6}$$

Another glycerol decomposition reaction is dehydration (Equation 2.7) which decomposes to glyceraldehyde (Equation 2.8). By elevated temperature, glyceraldehyde decomposes to 2-oxopropanal which then produces methane and carbon monoxide (Equation 2.9).

$$C_3H_8O_3 \rightleftharpoons C_3H_4O_2 + H_2O \tag{2.7}$$

$$C_3H_8O_3 \rightleftharpoons C_3H_6O_3 + H_2 \tag{2.9}$$

$$C_3H_4O_2 \rightleftharpoons CH_3CHO + CO \tag{2.8}$$

In addition to glycerol dehyration and dehyrogenation, decomposition to ethylene (Equation 2.10) also occurs. Beside ethylene, carbon monoxide and water are produced.

$$C_3H_8O_3 \rightleftharpoons C_2H_4 + CO + 2H_2O \quad \Delta H^0 = 251.2kJmol^{-1} \tag{2.10}$$

Coke formation occurs during glycerol dry reforming reaction which results in catalyst deactivation. It is also known that carbon decomposition is affected by reaction temperature (increased temperature hinders coke formation). According to Boudourad reaction (Equation 2.11), carbon formation increase at reduced temperatures. The other reactions leading to coke formation are given in Equations 2.12, 2.13 and 2.14 [33].

$$2CO \rightleftharpoons C_{(\mathrm{s})} + CO_2 \quad \Delta H^0 = -172.4kJmol^{-1} \tag{2.11}$$

$$CO_2 + 2H_2 \rightleftharpoons C_{(\mathrm{s})} + 2H_2O \quad \Delta H^0 = -90kJmol^{-1} \tag{2.12}$$

$$H_2 + CO \rightleftharpoons C_{(\mathrm{s})} + H_2O \quad \Delta H^0 = -131kJmol^{-1} \tag{2.13}$$

$$CH_4 \rightleftharpoons 2H_2 + C_{(\mathrm{s})} \quad \Delta H^0 = 74kJmol^{-1} \tag{2.14}$$

2.2.1. Thermodynamics

Glycerol dry reforming studies started in 2009 and first study was performed by Wang *et al.* [34] which was about thermodynamic investigation of glycerol dry reforming. In this study, Gibbs free energy minimization method was used and glycerol conversion was retained 100%. To calculate the equilibrium composition, Lagrange's undetermined multiplier method was used and three different parameters, namely temperature, pressure and CO_2 to glycerol ratio were examined. They found that increasing pressure affected hydrogen and syngas production negatively. So as to, atmospheric pressure was verified as optimum pressure value to produce highest amount of H_2 and syngas. They determined optimum conditions to produce optimum H_2 as 975 K temperature, the CO_2/Glycerol ratio range of 0-1 and atmospheric pressure. Optimum conditions to produce ultimate syngas were also detected and those were found as 1000

K and 1:1 CO_2/Glycerol ratio. At these conditions 33% CO_2 conversion was achieved while the obtained product (syngas) was 6.4 mol which was the maximum quantity. Moreover, carbon formation (which is not desirable) can be hindered from thermodynamic perspective but even if it cannot, thanks to and appropriate catalyst, carbon nanofilaments which are valuable product, can be obtained from GDR.

In the study of Kale and Kulkarni [35] thermodynamic study which was about glycerol dry autothermal reforming was carried out to determine process conditions for ultimate synthesis gas production. In this work, dry reforming and partial oxidation reactions were combined to supply energy from oxidation reaction which is exothermic to dry reforming reaction which is endothermic. Findings were gathered in the temperature range of 600-1000 K, O_2/C (carbon source is glycerol) ratio range of 0.1- 0.5 and CO_2/Glycerol ratio range of 1-5 at 1 bar constant pressure. The best thermoneutral point was observed at 926.31 K, 0.3:1 O_2/C and 1:1 CO_2/Glycerol ratios and 4.8 mol total hydrogen (which came from dry reforming and partial oxidation) was obtained.

Freitas and Guirardello examined and compared different glycerol reforming methods which are steam reforming, autothermal reforming, partial oxidation, supercritical water gasification and dry reforming in their studies [36]. For this purpose Gibbs free energy minimization method was used together with the virial equation of state to determine operational parameters namely temperature, pressure and feed composition. Carbon deposition was also investigated for all reforming technologies. The results showed that under the elevated temperature and decreasing pressure more H_2 and syngas were generated but H_2/CO ratio decreased for all examined technologies. Compared to others, highest syngas production (88.4%) with highest H_2 (61.9%) amount was achieved in steam reforming at 800°C, the lowest H_2/CO ratio which was 0.67 obtained in GDR technology. It was also found that pressure had negative effect on carbon formation in partial oxidation and dry reforming methods while there was no influence on others.

Lastly, Wang *et al.* [33] conducted another thermodynamic study which was about dry autothermal reforming of glycerol with *in-situ* H_2 separation. Gibbs free energy minimization method was used. Their results indicated that hydrogen removal boosted production of H_2 while inhibited the methane formation. H_2 separation also affected carbon formation especially lower CO_2/Glycerol ratios carbon deposition increased. By increasing temperature from 850 K to 900 K, thermoneutral O_2/Glycerol was also escalated from 0.15 to 0.4 because of H_2 separation. Hence, they found that removing H_2 helped to conduct autothermal reforming at high temperatures.

2.2.2. Catalysts

Glycerol dry reforming experimental studies started in 2010 and since then have drawn the attention of different experimental working groups. The work of Fernandez *et al.* [37] which was the first published article regarding this subject conducted glycerol pyrolysis, steam reforming and CO_2 reforming by using two different heating systems which are conventional (electrical system based) and microwave over activated carbon catalyst. In the article, those two technologies were compared and found that microwave heating system installation into dry reforming resulted in lower glycerol conversion and higher syngas yield compared to the conventional heating set up. Comparison of dry reforming and steam reforming showed that dry reforming had lower syngas quantity than steam reforming. Furthermore, carbon-based catalysts were found convenient for syngas production and minimizing CO_2 emission under the condition H_2/CO ratio ~ 1.

Lee *et al.* [7–9] published three successive articles about glycerol dry reforming over cement clinker-supported Ni catalysts between 2013 and 2014. In the first article [7], cement clinker (consists of 62% CaO and 17% SiO_2) supported Ni catalyst with different metal loadings (5, 10, 15, 20 wt.%) were prepared to prevent catalyst deactivation which comes from coke deposition. Therefore, with following characterization tests XRD, XRF, BET, TGA and FESEM-EDS, glycerol dry reforming performed on prepared catalysts under the conditions of 800° with different CO_2 partial pressure at $7.2x10^4$ mL g_{cat}^{-1} h^{-1}) gas hourly space velocities (GHSV). Results showed that with increasing Ni loadings, BET surface area were increased although cement-clinker had non-porous structure and this result was also confirmed by FESEM-EDS. According to activity results, the unity of CGR was the best condition to inhibit coke formation, other than 1 CGR (higher or lower) Boudouard reaction became dominant which resulted in coke deposition on catalyst. Later, to observe the effect of Ni loadings on activity, another study was performed in 2014 [8]. In that study, the catalysts which were consist of 62% cement clinker and 17% SiO loaded with different amount of Ni (growing weight percentage from 5 to 20) were prepared. Their findings showed that as Ni quantity increased, BET (specific surface area) increased from 0.55 to 17.83 m^2 g^{-1} and catalyst 20% Ni doping was the best option in terms of activity and selectivity during dry reforming reaction of glycerol. Syngas between 0.5-1.5 H_2/CO ratio (which is convenient for FTS) obtained under 800 K and CO_2/Glycerol ratio of 1. However, carbon formation (either whisker or graphitic type) was observed on 20% severely compared to other Ni loadings. Later in 2014, to specify optimum parameters, dry reforming reaction was performed over 20% Ni doped catalyst (which was found the best metal loadings in previous study) [9]. Reaction was performed in the temperature range of 923-1023 K and CO_2/Glycerol ratio range of 0.6-5 at 14 kPa constant glycerol partial pressure. Results showed that CO_2 and glycerol chemisorped at different active sites which was given rise to decomposition of glycerol predominantly. In consequence of activity tests, optimum conditions were determined as 973 K temperature and 1:1 CO_2/Glycerol ratio and as growing CO_2 /Glycerol ratio, glycerol conversion increased from 70% to 80% between 1 to 1.6 CO_2 /Glycerol ratio. This results showed that when H_2/CO ratio is less than 2, glycerol CO_2 reforming is applicable for Fischer Tropsch synthesis.

Siew *et al.* studied La-promoted Ni/Al_2O_3 catalysts over which dry reforming of glycerol performed comprehensively [10–13]. In the first study [11], the main focus was the characterization of the catalyst. To obtain significant results, two different catalysts which are La promoted and non-promoted were prepared by wet co-impregnation method. Their results showed that La-promoted catalysts had smaller crystalline size than non-promoted one which is also interpreted as higher metal dispersion and lower BET surface area due to pore blockage. After the characterization, dry reforming reaction was performed under the condition 873 K over 2% La-Ni/Al_2O_3 and 24.5% glycerol conversion with 9.7% H_2 generation were obtained. Later in 2014, catalytic study over

3% La-Ni/Al_2O_3 was carried out at 1023 K temperature and 1 atm pressure [10]. When CO_2/Glycerol ratio was differentiated between 0 to 1.7, the obtained H_2/CO ratios are between 0.8 to 2. They showed that that glycerol dry reforming reaction was feasible for gasoline production by means of FTS. In addition, XRD results showed that coke deposition occurred severely (33 wt.%) during dry reforming over virgin Ni/Al_2O_3 compared to La promoted since promotion enhanced redox capability of catalyst. One year later, over the same catalyst (3% La-Ni/Al_2O_3) dry reforming was performed by Siew *et al.* [13] in the temperature range of 700-900°C and CO_2/Glycerol ratio of 1-5. As the result of this work, 96% glycerol conversion was obtained at 1.67 CO_2/Glycerol ratio with H_2/CO ratio under 2 which is convenient for FTS. Based on experimental data, glycerol dry reforming kinetic model was also demonstrated by power law as shown below:

$$r_g = 2.6 \times 10^{-4} e^{\frac{-E_a}{RT}} (P_{C_3H_8O_3})^{\gamma} (P_{CO_2})^{\phi} \tag{2.15}$$

Siew *et al.* [12] also investigated longevity of the La-promoted Ni/Al_2O_3 catalyst and their findings showed that 3 wt.% La-Ni/Al_2O_3 had the largest BET specific surface area which is 97m^2.g^{-1}. Moreover, it was determined as the best service of life without any degradation (above 90% conversion) and the most stable even after 72 h resistance time. It was also seen that existence of CO_2 lessens the coke deposition by means of gasification reaction.

In 2016, Arif *et al.* investigated effect of support and metal loadings on glycerol reforming [14]. For this purpose, two different support which are ZrO_2 and CaO and different Ni loadings (5, 10, 15 wt.%) were tested at 973 K and 1:1 CO_2/Glycerol ratio under 1 atm over 3 hours. According to their findings, 15% Ni/CaO had better activity performance (24.59% hydrogen yield and 30.32% glycerol conversion) compared to other catalysts. Considering XRD analysis, 5% Ni/CaO had smaller crystallite structure and smoothly dispersed Ni particles which leaded higher specific surface area. One year later Arif *et al.* [15] conducted another study about glycerol dry reforming over Ni catalysts with different supports. In this work, Ni amount fixed to 15% and CaO, ZrO_2 and La_2O_3 were used as support. Reaction conditions of previous study was also used in this study. According to results, Ni/CaO had better catalytic performance which come from higher specific surface area compared to other catalysts. The effect of temperature and CO_2 to glycerol ratio were also investigated and it was seen that optimum parameters were determined as 1073 K and 1:1 CO_2/Glycerol ratio. At these condition 37.6% glycerol conversion and 32.4% H_2 were obtained. In the recent study of Arif *et al.* [16], the effect of Re addition to Ni/CaO catalyst (which had superior catalytic performance was proven in the previous studies) was investigated. Experiments were performed in the CO_2/G range of 1-5 , temperature range of 873-1173 K and gas hourly space velocities (GHSV) range of 1.44 x 10^4-7.2 x 10^4 mL g_{cat}^{-1} s^{-1}. While optimum operating temperature and GHSV for promoted and unpromoted catalysts were determined as 800 K and 3.6 x 10^4 mL $g^{-1}{}_{cat}$ s^{-1}, CO_2 to glycerol ratio was identified as 1 for Ni/CaO and 3 for Re-Ni/CaO. Furthermore, 5%Re- Ni/CaO had better glycerol conversion and H_2 yield of 61% and 56%, respectively. Addition of Re increased acidic sites which helped glycerol to adsorbed by active sites. Therefore, more glycerol reacts with more CO_2 and glycerol conversion increases. It was also found that CO_2 partial pressure did not have significant effect on glycerol conversion and H_2 yield. According to characterization results, whisker type carbon deposition was not prevented but with addition of Re it was able to be reduced.

In the study of Harun *et al.* [17], different amount of Ag promoted Ni/SiO_2 catalysts were prepared by wet impregnation method and dry reforming reaction conducted over those catalysts at 973 K and 1:1 CO_2/Glycerol ratio under 1 atm. According to their findings, Ag(5)-Ni/SiO_2 (which possesses maximum Ag loadings) had the highest glycerol conversion and H_2 production 32.6% and 27.4% respectively. Characterization results also showed that Ag promotion enhanced NiO dispersion which explained high conversion of Ag(5)-Ni/SiO_2. Later, Harun *et al.* [18] synthesized Ni with two different supports which are Al_2O_3 and SiO_2 to observe effect of support on glycerol dry reforming. Reaction was conducted at 973 K under 1 atm. Compared to Ni/SiO_2, Ni/Al_2O_3 had better glycerol conversion and H_2 production (14.46% and 9.82%, respectively). These superiority resulted from higher specific surface area, smaller particle size, higher acidic property and stronger support metal interaction of Al_2O_3. For both catalysts whisker and encapsulating type carbon can be observed but those carbon structures can be eliminated *via* oxidation. In the most recent study of Harun *et al.* [19] focused on glycerol dry reforming over Ag-promoted and unpromoted Ni/Al_2O_3 catalyst under different temperatures (varying from 873 K to 1173 K), different gas hourly space velocities (GHSV) (varying between 14.4 and 72 L g^{cat-1} h^{-1}) and different CO_2/Glycerol ratios (varying between 0.5 and 5). According to their results the highest glycerol conversion and H_2 yield (40.7% and 32% respectively) obtained at 1073 K, 36 L g^{cat-1} h^{-1} GHSV and 1:1 CO_2/Glycerol ratio over Ag(3)- Ni/Al_2O_3. By increasing Ag loadings resulted in catalysts deactivation since smaller particles covered active sites. Moreover, Ag(3)- Ni/Al_2O_3 catalysts possessed smaller metal crystallite size which associated also smooth metal dispersion. Stability tests results showed that catalysts was stable during 72 hours time on stream. Characterization results showed that carbon deposited in the form of whisker and encapsulated but former type can be wiped out by oxidation.

In 2018, Tavanarad *et al.* published two articles [20, 21]. In the first [20], glycerol dry reforming reaction was performed over a series of mesoporous Ni (5, 10, 15, 20 wt.%) supported by γ-Al_2O_3. By increasing Ni loading from 5 to 20% resulted in a decrease on BET surface area (from 180 to 143 m^2 g^{-1}) and an increment on Ni crystalline size from 6.6 to 19 nm. While Elevating GHSV caused a decrease on glycerol conversion, the increase of CGR resulted in more coke deposition on catalyst surface. Among the prepared catalysts, 15% Ni/γ-Al_2O_3 exhibited best catalytic performance. However, during 20 h on stream stability tests at 700°C, activity decreased significantly in 5 hours and than stabilized. In the second article [21], they focused on noble metals nanocatalysts such as Rh, Ru, Ir, Pd and Pt supported on Mg/Al_2O_4 and glycerol dry reforming reaction was performed over all those prepared catalysts. The BET analysis showed that specific surface area of Rh, Ru and Pd were higher than other noble nanocatalysts. According to activity test results, under CGR of 1, Rh had better activity and stability performance which was associated to its higher specific surface area and more active sites. Activity results also showed that increasing CO_2 to glycerol ratio 0 to 3 enhanced catalytic activity and reduced coke deposition and by increasing GHSV 3 times at 973 K, glycerol conversion declined to 42.9% from 97.5%. 20 h on stream stability test of Rh/$MgAl_2O_4$ performed at 973 K and 1 CGR and decline on activity and severe coke deposition through 14 h were observed and activity immobilized after 14th hours.

Bulutoglu and co workers conducted a study [22] about glycerol dry reforming over Rh/ZrO_2 and Rh/CeO_2 to observe effect of feed composition and temperature on activity and stability performance. This study brought new perspective to literature due to characterize both fresh and used catalysts and report CO_2 conversion. Activity results showed that both ZrO_2 and CeO_2 supported catalysts exhibited excellent activity performance along with increasing temperature and CO_2 conversion above 700°C. With elevating temperature, H_2/CO ratio came up to 0.8 which is suitable for Fisher Tropsch synthesis and carbon deposition lessened with increasing temperature. Compared to Rh/CeO_2, Rh/ZrO_2 had marginally higher surface area and smaller Rh-particle size which contributed its activity performance positively. Characterization results also showed that Rh/CeO_2 had strong support-metal interaction which resulted in Rh metal particles encapsulation. Therefore, Rh metal activity restrained by CeO_2 support. On the other hand, strong support-metal interaction increased stability performance of Rh/CeO_2 at 750°C temperature and 4 CGR. This is because, CeO_2 had oxygen vacancies which helped to remove carbon which deposited on active sites. In the case of Rh/ZrO_2, Rh metal particles was sintered which resulted in deactivation of catalyst.

Lastly, in the study of Bac *et al.* [38], glycerol dry reforming on Rh, Ni and Co supported by Al_2O_2-ZrO_2-TiO_2 (AZT) was performed between 600-750°C and 1-4 molar CO_2/G ratio. Results showed that Ru/AZT had the best activity performance and followed by Ni/AZT and Co/AZT. By increasing residence time, Rh/AZT achieved 90% of thermodynamic equivalent at 750°C and CO2/G=2-4 at which Ni/AZT enhanced to 95% of its thermodynamic limit. The longevity study showed that with nearly 13% activity loss, Ni/AZT and Rh/AZT had the best stability performance while Co/AZT showed poor stability performance due to carbon formation, sintering and oxidation of CO sites, which were exhibited by TEM-EDX, XPS, XANES and *in-situ* FTIR anaylsis. On the other hand, Rh/AZT had no deactivation indication according to characterization tests while Ni/AZT revealed gasified carbonaceous deposits in the early part of the reaction.

2.3. Ni/La_2O_3-ZrO_2 Binary Oxide Support

Mixed oxides ensure superior catalytic performance since they have a combination of constituent oxides properties. In the literature, those supports have been entreated and used reforming reaction studies extensively. In recent years, La_2O_3-ZrO_2 has been regarded as promising alternative to binary oxide support.

In 2012, Sokolov *et al.* [39] published an article about low-temperature methane dry reforming over mesoporous Ni/La_2O_3-ZrO_2 catalyst. Findings show that, Ni/La_2O_3-ZrO_2 had high CO and H_2 yields which was nearly thermodynamic limit. Beside good catalytic activity, it also showed superior stability performance. In the course of the study, different pore size catalysts were prepared and characterization tests of fresh and used catalyst were performed. These results showed that the activity mesoporous Ni/La_2O_3-ZrO_2 catalyst did not change over 180 hours on stream experiment while others deactivated. According to examination of deactivated catalysts, deactivation occurred due to graphene type carbon deposition and NiO formation on Ni particles. The superior stability of Ni/La_2O_3-ZrO_2 was attributed to strong support - active metal interaction *via* arrangement of pore size.

Xue and co-workers conducted a study about acetic acid steam reforming over Ni/La_2O_3-ZrO_2 catalyst [40]. In this study, experiments were performed at the temperature range of 550-750°C. It was observed that Ni particles were smoothly dispersed on the support surface. In addition, at 600°C, 89.27% CO and 80.41% H_2 yields were achieved. This great activity performance was attributed to high BET surface area and strong metal-support interaction. Lastly, 15 wt.% Ni/La_2O_3-ZrO_2 catalyst achieved superior stability performance over 20 hours period.

In the study of Angeli *et al.* [41], low temperature steam reforming reaction was performed over Rh and Ni active metals which were impregnated on La_2O_3-ZrO_2 and

La_2O_3-CeO_2-ZrO_2 supports and three distinct parameters (temperature, GHSV and H_2O/CH_4 ratio) were investigated. Beside activity test, stability examination is also performed over 90 hours period and catalyst predisposition to carbon deposition was also investigated. According to stability test, findings showed that Ni(10)/CeZrLa has better performance thanks to Ce addition to support which eliminated coke deposition due to supplying active oxygen. La addition also stabilized the catalyst and improved coke resistance. According to TPO and TPH analysis, deposited carbon is highly active which can be removed *via* oxidation and hydrogenation and this feature makes Ni(10)CeZrLa a promising catalyst.

Li and co-workers published an article about methane dry reforming over Ni/La_2O_3 [42]. They found that La_2O_3 support dispersed Ni particle smoothly on its surface. Moreover, nanorod support structure ensured basic sites which enhances CO_2 adsorption and activation of catalyst. According to activity results, 70% methane conversion, 75% CO_2 conversion and H_2/CO ratio of 0.87 were achieved at 973 K over 50 hours period. Coke deposition over catalyst was also examined and it was seen that coke dissociation is affected by Ni dispersion.

In the study of Goula [43] , methane CO_2 reforming over Ni/ZrO_2, Ni/La_2O_3-ZrO_2 and CeO_2-ZrO_2 catalyst was performed distinctively. Study was performed at 500-800°C temperature range and 1.5 CH_2/CO_2 of 1.5 ratio. Results shows that Ni/LaZr and Ni/CeZr had better catalytic as well as stability performance than Ni/Zr since Ce and La had basic structure and oxygen capacity which inhibits carbon formation on catalyst surface. Beside activity and stability studies, characterization tests were also applied to fresh and used catalyst. According to results, Ni/LaZr and Ni/Zr had predisposition to form filamentous type carbon on catalyst surface. On the other hand, Ni/CeZr showed trace amount of carbon formation on its surface.

Methane dry reforming over Ni-Mo_2C/La_2O_3-ZrO_2 was performed by Tao and co-workers [44]. In the content of this study, methane dry reforming was conducted at the 973-1173 K temperature range in the fixed-bed reactor. It was seen *via* characterization tests that La_2O_3-ZrO_2 has oxygen vacancies which accelerates dry reforming reaction.

At 900°C, 94% of methane conversion was achieved and catalyst shows superior stability performance over 100 hours period. This remarkable stability and activity performance was attributed to the enhanced BET surface area together with small crystal size.

Cheng *et al.* [45] conducted coke oven gas dry reforming over Ni/La_2O_3-ZrO_2 catalyst prepared by different methods. In this study, the effect of La loading on activity was also investigated. It was seen that all prepared catalysts exhibited good activity performance as well as low coke deposition on active sites. Among all prepared catalysts, 8% Ni/La_2O_3-ZrO_2 prepared by sol-gel method had superior activity thanks to its good pore size.

3. EXPERIMENTAL WORK

3.1. Materials

3.1.1. Chemicals

Chemicals which were used as catalyst are listed in Table 3.1. ZrO_2 (Zr) and La_2O_3 (La) were used as support and $Ni(NO_3)_2.6H_2O$ was used as active metal. Deionized water was supplied by Zeneer Water Purification System with above 0.1 μS cm^{-1} conductivity.

Table 3.1. Chemicals used in catalyst preparation.

Chemicals	**Formula**	**Supplier**	**MW (g mol^{-1})**	**Purity**	**Usage**
Zirconium oxide	ZrO_2	Alfa-Aesar	123.22	-	Support
Lanthanum(III) oxide	La_2O_3	Sigma-Aldrich	325.81	99.99%	Support
Lanhania-Zirconia	La_2O_3-ZrO_2	Daichi Kigenso	405.36	-	Support
Deionized water	H_2O	-	18.02	-	Solvent

3.1.2. Gases and Liquids

Table 3.2 and Table 3.3 involve all gases and liquids which were used in experimental system, respectively. Only Ar and He were used as carrier gases of gas chromatographs (GCs) and other gases were used for GC calibration. H_2 was also used for catalyst reduction. In the experiment, N_2 was used as inert and CO_2 was used as gaseous reactant. Glycerol was used as liquid reactant and its specifications are listed in Table 3.3. Other liquid chemicals (distilled water, ethanol and acetone) which are listed in the table are used for cleaning.

Table 3.2. Gases used in the experimental system.

Gas	Specifications	Application
Argon	99.998%	GC carrier gas
Carbon dioxide	99.995%	GC calibration, reactant
Carbon monoxide	99.90%	GC calibration
C_2 mixture	2% C_2H_6, 2% C_2H_4, 5% CH_4, balance N_2	GC calibration
Helium	99.99%	GC carrier gas
Hydrogen	99.99%	GC calibration, reducing agent
Methane	99.50%	GC calibration
Nitrogen	99.998%	GC calibration, inert

Table 3.3. Liquids used in the experimental system.

Liquid	Formula	Supplier	MW (g mol^{-1})	Purity	Usage
Glycerol	$C_3H_8O_3$	Sigma-Aldrich	92.09	> 99.5%	Reactant
Ethanol	C_2H_5OH	Merck	46.07	> 99.9%	Cleaning
Acetone	C_3H_6O	Merck	58.08	> 99.8%	Cleaning
Distilled Water	H_2O	-	18.02	-	Cleaning

3.2. Experimental System

Experimental system of this study contains 3 main parts:

- Catalyst Preparation System: Incipient-to-wetness impregnation method was used to prepare catalysts. To apply this method, precursor solution (which is in

Buchner flask) was added drop-wise on support by means of a peristaltic pump. This procedure was carried out in ultrasonic mixer to ensure optimum mixing.

- Catalytic Reaction System: The reaction performed in a packed-bed reactor along with mass flow controllers and HPLC pumps to feed reactants in a controlled manner. Reaction temperature was altered by temperature controllers which were located in the three zone furnace.
- Product Analysis System: The reactor exit stream was sent to two gas chromatographs (GC) to inspect product composition.

3.2.1. Catalyst Preparation System

Catalysts which were used in this study were prepared by incipient-to-wetness impregnation method and it was presented in Figure 3.1. Before impregnation, KNF diaphragm vacuum pump moved air away from the pores of support. Then, Masterflex peristaltic pump was used to add precursor to support. After impregnation, support-precursor mixture was mixed properly and continuously by means of Retsch UR1 ultrasonic mixer. In Section 3.3 comprehensive explanation of catalyst preparation was taken place.

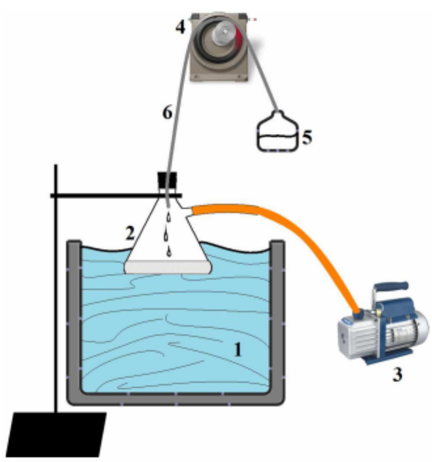

Figure 3.1. Exemplification of catalyst impregnation system *via* incipient-to-wetness impregnation [3–5]. 1. Ultrasonic Mixer, 2. Buchner Flask, 3. Vacuum Pump, 4. Peristaltic Pump, 5. Precursor Solution, 6. Silicon Tubing.

3.2.2. Catalytic Reaction System

The reaction system consists of 3 main divisions: feed, reaction and product analysis. Those three parts are represented in Figure 3.2 and the system can also viewed in Figure 3.3.

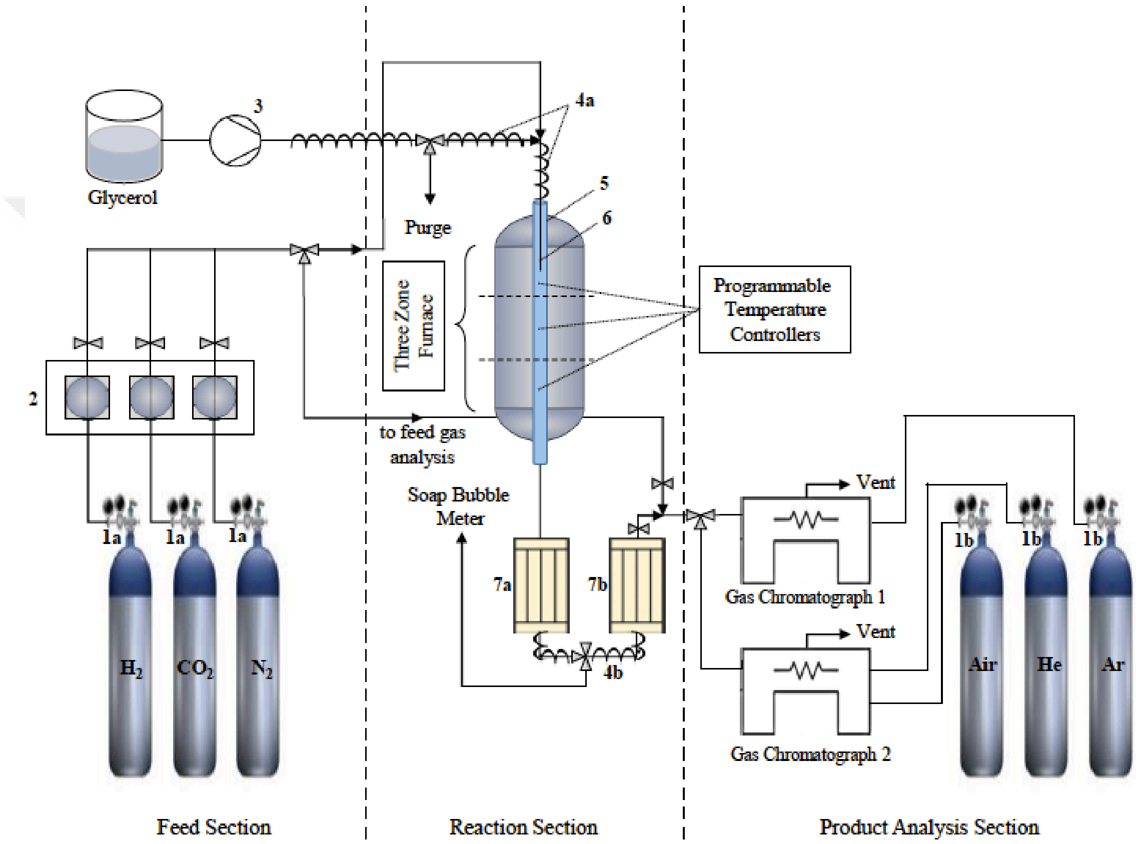

Figure 3.2. Demonstration of the experimental system.

<u>3.2.2.1. Feed Section.</u> The feed section shown in Figure 3.2 is composed of high-performance liquid chromatography (HPLC) pump to feed glycerol into system and Brooks Model 5850E series mass flow controllers (MFC) to feed and adjust N_2, H_2, CO_2 from pressurized storage tanks by means of regulators (supplied from Linde Group). Connections were established by Swegelok tubing and fitting in three sizes: 1/4”, 1/8” and 1/16”.

Outlet pressures of N_2, H_2 and CO_2 storage tanks were kept at about 2 atm through regulators and the other end of those regulators were connected to MFCs *via*

Figure 3.3. Pictorial representation of experimental set-up.

1/8” tubing. All MFCs were controlled by the same Brooks Instruments MFC display box. Calibrations of MFCs were done and actual flow rates and corresponding set points are shown in Appendix A. There are on-off valves at the end of each MFC just in case back flow of reactant-product stream occurs. Then, outlets of three MFC were reduced from 1/4” to 1/8” by means of reducing union which was located before three-way valve. Three-way valves were provided to alter the direction of feed gas which can be sent either to the reactor or to gas chromatographs to analyze feed composition. Right before entering the reactor, tubing size was reduced from 1/8” to 1/16”.

Glycerol was sucked from 50 mL graduated cylinder by means of HPLC pump and fed into reactor through 1/16” tubing around which a heating line was wound. Heating process must be done to facilitate flow of glycerol which has quite high viscosity. Heating line temperature was set at $\sim$100°C *via* ENDA ET4420 digital proportional integral derivative (PID) controller. Exit pressure of HPLC pump was around 3 bars which is displayed on the HPLC screen.

Glycerol and gaseous feed were jointed immediately before entering the reactor by means of union tee and led into the reactor through 1/16" tubing which is named injector. According to calculations, 10 cm injector length is enough to vaporize glycerol completely (shown in Figure 3.4). Temperature of reactor top was also kept over 400°C to ensure all reactants in gaseous phase. To establish desired CO_2/Glycerol ratio, it was proven by our research group that this configuration is the best alternative [3, 4].

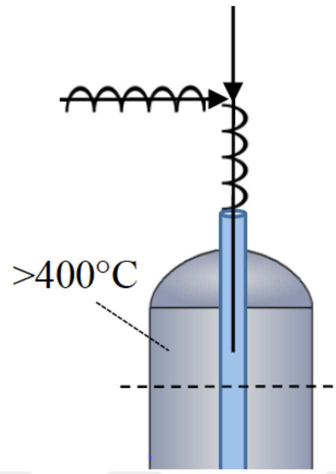

Figure 3.4. Detailed representation of reactor inlet.

3.2.2.2. Reaction Section. The reaction section contains PROTHERM PZF 12/50/500 three zone furnace whose temperature is controlled by PC442 PID controller, quartz reactor and two cold traps in Dewar flasks as shown in Figure 3.2.

Quartz reactor whose length is 80 cm was used as packed bed reactor, as explained in detail in Section 3.5. While the middle zone of furnace was kept at reaction temperature, temperature of top and bottom zone were intended to stay above 400°C which is higher than glycerol boiling point (Glycerol boiling point:310°C).

Outlet of reactor was followed by two successive cold traps in ice-filled Dewar flasks. By this set-up, condensation of low boiling point hydrocarbons and water was aimed for. The flow which arrives the outlet of the first cold trap was sent to either soap bubble meter to measure actual flow rate in the system to prevent any gas leakage or to the second cold trap by means of three-way valve. Soap bubble meter opened to vent. Likewise, winding heating line around glycerol tubing, 1/8" tubing which

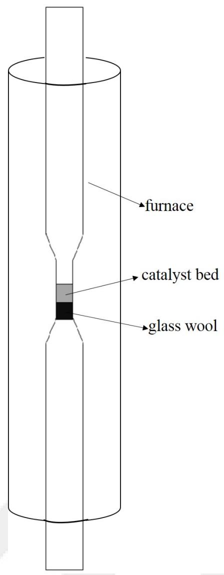

Figure 3.5. Depiction of packed bed reactor.

was located between two cold traps was also wound around and heated at ∼ 120°C to prevent any blockage caused by condensed products. In the end of the second cold trap, gaseous products arrived in product analysis system.

3.2.2.3. Product Analysis Section. Product analysis section contains two gas chromatographs, He, Ar and dry air storage tanks. Necessary information about gas chromatographs and analysis details took place in Section 3.2.3. Product and feed gaseous were connected by three-way valve before entering gas chromatographs and direction of three-way valve determines which gas analyzes. Three-way valve was also connected to another three-way valve which directs stream to intended chromatographs.

3.2.3. Product Analysis System

To determine the composition of feed and product stream, product analysis system was used. Streams were analyzed by two gas chromatographs which are Shimadzu GC-2104 (GC1) and Agilent 6850N (GC2). They analyze different compounds and their specifications are listed in Table 3.4. Their calibration graphs can also be found in Appendix A and those charts were generated to attain which flow rate of particular compounds is corresponding to which peak collected from GCs. While carrier gas of

Shimadzu GC-2104 is Ar, of Agilent 6850N is He and those carrier gases was connected to GCs through 1/8” tubing. Their regulator pressures were altered to about 6.5 atm. To send exact volume of stream to analyze, a pneumatic valve was used in GC2, while it was done manually in GC1 and to switch pneumatic valve on and off, dry air was also connected to GC2.

3.3. Catalyst Preparation and Pretreatment

There different catalysts which are Ni/La_2O_3, Ni/ZrO_2 and Ni/La_2O_3-ZrO_2 were used in this work. Catalyst preparation section included preparation of support, catalyst synthesis by incipient-to-wetness impregnation and catalyst pretreatment *via* H_2.

3.3.1. Preparation of Support

3.3.1.1. Preparation of ZrO_2. The size of ZrO_2 whose qualifications are listed in Table 3.1 was reduced to 45-60 (250-354 μm) mesh *via* sieve. Then, it was calcined for 4 hours under H_2 flow at 800°C.

3.3.1.2. Preparation of La_2O_3. La_2O_3 whose qualifications are listed in Table 3.1 was calcined for 4 hours under H_2 flow at 800°C.

3.3.1.3. Preparation of La_2O_3-ZrO_2. La_2O_3-ZrO_2 whose qualifications are listed in Table 3.1 was calcined for 4 hours under H_2 flow at 800°C.

3.3.2. Preparation of Active Catalyst

3.3.2.1. Preparation of Ni/ZrO_2. To prepare 1 gram of 5 wt.% Ni/ZrO_2, 0.2477 gram of Ni precursor was weighed and dissolved in $\sim$ 1.3 mL deionized water. In the meantime, 0.95 gram of ZrO_2 was weighed and stirred *via* ultrasonic mixer under vacuum for about 30 minutes to get rid of air in the pores. 30 minutes later, Ni precursor was added drop-wise to the ZrO_2 support by means of peristaltic pump whose velocity was

Table 3.4. Operating parameters of gas chromatographs.

GC Parameter	Schimadzu GC-2014 (GC1)	Agilent 6850N (GC2)
Compounds	H_2, N_2, CH_4, CO	CO_2, C_2H_6, C_2H_4
Carrier gas	Argon	Helium
Carrier gas flow rate (mL min^{-1})	25	20
Column ID (mm) and length (m)	2.1 & 2.0	2.1 & 1.82
Column oven temperature (°C)	50	40
Column packing material	Molecular Sieve 5A (60-80 mesh)	Porapak Q (80-100 mesh)
Column tubing material	Stainless steel	Stainless steel
Detector current (mA)	50	Set by GC itself
Detector temperature (°C)	150	80
Detector type	Thermal conductivity	Thermal conductivity
Injector temperature (°C)	80	90
Sampling loop volume (mL)	1.3	1

adjusted to 0.04 m s^{-1}. The slurry form of support-precursor combination was mixed for 1.5 hours to disperse Ni particles on ZrO_2 well enough. Later, the prepared catalyst was dried at 110°C overnight then calcined at 800°C in the presence of air.

3.3.2.2. Preparation of Ni/La_2O_3. To prepare 1 gram of Ni/La_2O_3 catalyst, the same procedure clarified in Section 3.3.2.1 was followed. Only dissolution of Ni precursor in deionized water was carried out in $\sim$ 0.65 mL of water.

3.3.2.3. Preparation of Ni/La_2O_3-ZrO_2. To prepare 1 gram of Ni/La_2O_3-ZrO_2 catalyst, the same procedure as clarifies in Section 3.3.2.1 was followed. Only dissolution of Ni precursor in deionized water was carried out in $\sim$ 0.7 mL of water.

3.3.3. Pretreatment of Catalysts

To reduce metal oxide sites, all prepared catalysts were heated up to 800°C under N_2 flow. When the temperature reached 800°C, 40 NmL of H_2 was treated to catalyst loaded reactor for 2 hours before starting the experiments. Later, the reactor was cooled down to experiment temperature under N_2 flow.

3.4. Reaction Tests

In this study, a quartz reactor whose length is 80 cm was used. Its inner diameter is 2 cm at the ends and narrows down to 1 cm in the middle. As shown in Figures 3.5 and 3.6, 1 cm of quartz wool was packed into the middle of the reactor. Then, $\sim$1 cm of catalyst and α- Al_2O_3 (as dilution) mixture was placed on quartz wool. While 20 mg catalyst mixed with 720 mg of Al_2O_3 in activity tests, 150 mg catalyst without any dilution was used in stability tests. This configuration was applied to provide that bed length/particle diameter and tube diameter/particle diameter ratios are approximately 35 which is an assumption of plug flow to neglect diffusion limitations [46].

Figure 3.6. Catalyst packed quartz reactor.

3.4.1. Activity Tests

In the content of activity test, the effect of different parameters which are temperature, CO_2/Glycerol ratio and W/F ratio on glycerol conversion, CO_2 conversion and product distribution were examined. While performing experiments, glycerol feed and gaseous flow rate were fixed to 4 NmL min^{-1} and 40 NmL min^{-1}, respectively. To set desired CO_2/Glycerol ratio, CO_2 flow rate was altered and N_2 flow was adjusted according to CO_2 flow rate by keeping the total flow constant. The range of parameters and default values are listed in Table 3.5. When a parameter was investigated, other parameters and default values were kept constant. The experiment lasted 5 hours. First data was taken at 30th minute and then data collection period was extended to 45 minutes.

3.4.2. Stability Tests

In the content of stability test, the deactivation of catalyst over the time was investigated. Therefore, 72 hours on-stream experiment was carried out at 750°C, CO_2/Glycerol ratio of 2 and W/F ratio of 3.75 mg min NmL^{-1}. Within the first 5 hours data was taken in the same procedure with activity experiments. After 5 hours, data collection period was extended from 45 minutes to 1 hour until 7th hour data.

Table 3.5. Reaction conditions and parameters for experiments.

Parameter	Value
Reaction Temperature (°C)	700, 750
Glycerol Flow Rate (NmL min^{-1})	4
CO_2/G Feed Ratio	1, 2, 3, 4
Catalyst Amount (mg)	20, 50, 100, 150
Total Flow Rate (NmL min^{-1})	40
W/F (mg min NmL^{-1})	0.5, 1.25, 2.5, 3.75

After 7th hour data, the period was extended to 2 hours. Last three data (70th and 71th and 72th hour data) was collected again in 1 hour period and the experiment was finished at the 72th hour. If CO_2 conversion was zero before the 72th hour, the experiment was finished at that time.

3.4.3. Experimental Procedure

The experimental procedure proceeds as follows:

- Quartz wool and prepared catalyst (with or without dilution) are placed in quartz reactor.
- The reactor is stored in the furnace.
- Leakage test is done. To do this, 20 NmL min^{-1} of N_2 is flowed through the reactor, and the exit of the reactor is directed to the vent.
- Middle zone temperature controller of furnace is set to 800°C.
- When the temperature is 800°C, 40 NmL min^{-1} H_2 is sent to the reactor for 2 hours and immediately after that, N_2 flow is closed. In meantime, GC1 and GC2 are turned on and operating conditions (shown in Table 3.5) are set.
- When 2 hour reduction comes to end, H_2 flow is closed and N_2 is set to the value that should be in the experiment and flowed through reactor.

- Furnace is set to the temperature at which the experiment is performed. In the meantime, two heating lines are also switched on.
- When the temperature of heating lines and furnace are reached to their set points, ice cubes are placed in two successive Dewar flasks. HPLC pump is switched on and glycerol is sent to purge. When the first drop is seen in the purge, glycerol valve is turned from purge to the system.
- CO_2 is set to the value that should be in the experiment and, 2 minutes later, CO_2 is sent into the reactor. At that moment, experiment period is started and the reactor outlet is directed to GCs from vent.
- The first data is taken at 30^{th} minute and then data collection period is extended to 45 minutes.
- Since it takes time to arrive effluent to the GC2 (GC2 is located after GC1), first data is taken from GC2 and, immediately after GC2 data collection, GC valve is turned to GC1 direction to take data from GC1. 2.5 minutes are waited to ensure that accurate sample mixture arrives to the GC1. 2.5 minutes later, the data is collected from GC1 and the valve is turned back to GC2.
- At the end of 5 hours, temperature controllers of furnace and heating lines are turned off. HPLC pump is switched off and glycerol valve is turned to the purge. Exit of reactor is directed to the vent. N_2 flow rate is set to the value required for feed gas analysis and feed stream is sent directly to the GCs, thus bypassing the reactor.
- Roughly 15 minutes later, feed gas analysis is done at GC2.
- When data collection is finished, CO_2 flow is turned off and N_2 flow rate is set to 20 NmL min^{-1}.
- The reactor is cooled to room temperature overnight with the presence of N_2 flow. When GCs analysis finish, their detectors are switched off and they are also cooled.
- When Detector temperature of GCs is above 100°C, GCs are switched off.

3.4.4. Measurement of Catalytic Activities

In this work, the effects of temperature, residence time and CO_2/Glycerol ratio on product distribution, CO_2 conversion, glycerol conversion, activity loss and selectivity were examined.

$$x_{CO_2} = \frac{F_{CO_{2,in}} - F_{CO_{2,out}}}{F_{CO_{2,in}}} \tag{3.1}$$

In order to calculate CO_2 conversion, Equation 3.1 was used. Although calculation of CO_2 conversion is simple, many side reactions and their products make glycerol conversion calculation complicated. Since only gaseous product can be analyzed in GC instruments, liquid products are condensed *via* cold trap and so their contribution to glycerol conversion is neglected. For this reason, it would be appropriate to name glycerol conversion as glycerol conversion to gaseous products. However, to simplify the definition, glycerol conversion is still used. To calculate glycerol conversion, H atom balance was applied and supposed that only H source is glycerol in the feed stream. Eventually, glycerol conversion equation was formed according to compounds which contain hydrogen and detected by GCs and it was calculated by using Equation 3.2:

$$x_G = \frac{2F_{H_2} + 4F_{CH_4} + 4F_{C_2H_4} + 6F_{C_2H_6}}{8F_{G,in}} \times 100 \tag{3.2}$$

Since there many reactions takes place during the glycerol dry reforming, yield and selectivity calculations become very important. Those parameters were calculated as shown in Equation 3.3 and Equation 3.4, respectively. While moles of glycerol fed into the system were based on yield calculation (Equation 3.3), moles of glycerol converted into product were based on selectivity calculation (Equation 3.4).

$$Y_i = \frac{F_{i,out}}{F_{G,in}} \tag{3.3}$$

$$S_i = \frac{F_{i,out}}{x_G F_{G,in}} \tag{3.4}$$

4. RESULTS AND DISCUSSION

In this study, the effects reaction temperature, CO_2/G ratio and residence time on catalytic performance were studied extensively. In addition, stability tests were performed to observe catalyst deactivation over time.

4.1. Effect of CO_2/Glycerol ratio

Regarding glycerol dry reforming, CO_2/G ratio has profound impact on reaction rate, according yields (CO_2 and glycerol) and product distribution. To observe CO_2/G ratio effect comprehensively, activity tests were performed at four ratios, 1 to 4 while total flow rate and glycerol feed were fixed to 40 and 4 NmL min^{-1}, respectively. In order to determine thermodynamic limits, thermodynamic analyses were done by using Gibbs free energy minimization method with respect to CO_2/G ratio.

4.1.1. Thermodynamic analysis

To specify thermodynamic limits, CHEMCAD 7.1.4 software was used. In the software, Gibbs free energy reactor was established and reactants flow rates which correspond to the current CO_2/G values were entered. As a requirement of the methodology, all possible compounds needed to introduce to the software. In glycerol dry reforming case, possible products are $C_3H_8O_3$, CO_2, N_2, H_2, CO, H_2O, CH_4, C_2H_4, C_2H_6, C_3H_4O, C_2H_4O, C_2H_6O, C_3H_6O and $C_{(s)}$. Another important point is contact time of reactant-product and catalyst which needs to be long enough. Therefore, W/F ratio approaches infinity. After making necessary arrangements, the reactor temperature was kept at 750°C and four different CO_2/G ratios were entered to the software.

In Table 4.1 and Table 4.2, yield and selectivity values of products are presented respectively. When the tables are examined in detail, only five possible products data were tabulated because selectivity of others which were not tabulated are equal to zero. That means they are not thermodynamically favored.

Table 4.1. Thermodynamic product yields at four CO_2/G ratios at 750°C.

$\mathbf{CO_2/G}$	$\mathbf{Y_{H_2}}$	$\mathbf{Y_{CO}}$	$\mathbf{Y_{CO_2}}$	$\mathbf{Y_{CH_4}}$	$\mathbf{Y_{H_2O}}$	$\mathbf{H_2/CO}$	$\mathbf{x_{CO_2}(\%)}$	$\mathbf{x_G(\%)}$
1	3.49	3.40	0.57	0.03	0.46	1.02	43.02	88.55
2	3.17	3.78	1.22	0.01	0.80	0.84	39.32	79.95
3	2.90	4.07	1.93	0.01	1.08	0.71	35.71	72.94
4	2.68	4.30	2.69	0.01	1.31	0.62	32.69	67.17

Table 4.2. Thermodynamic product selectivities at four CO_2/G ratios at 750°C.

$\mathbf{CO_2/G}$	$\mathbf{Y_{H_2}}$	$\mathbf{Y_{CO}}$	$\mathbf{Y_{CO_2}}$	$\mathbf{Y_{CH_4}}$	$\mathbf{Y_{H_2O}}$
1	3.94	3.84	0.64	0.03	0.52
2	3.97	4.72	1.52	0.02	1.00
3	3.98	5.58	2.65	0.01	1.48
4	3.98	6.41	4.01	0.01	1.96

Another point is that complete glycerol conversion has to be 100% since there is no glycerol in the reactor effluent. However, as explained in Section 3.4.3, glycerol conversion to gaseous product was reported throughout this study and so thermodynamic limits are different from 100%. In the study of Wang *et al.* [34], Gibbs free energy minimization study was conducted and complete glycerol conversion was accounted.

Thermodynamic analysis showed that increasing CO_2 quantity in the feed stream inhibits CO_2 conversion as well as glycerol conversion. It also affected H_2/CO ratio negatively since H_2 exhibits decreasing behavior while CO does exact opposite attitude. This is because increasing CO_2 amount gives rise to syngas selectivity in that way shifting the WGS reaction to opposite direction in which H_2 is consumed while CO is produced. Therefore, H_2/CO ratio declines with increasing CO_2/G ratio and this relation was already reported in previous studies [34,36]. Methane, which is undesirable product in glycerol dry reforming, was also affected by CO_2/G ratio. By increasing CO_2/G ratio, CH_4 amount in product composition was reduced.

4.1.2. Activity Tests

CO_2/G ratio-dependent variations of CO_2 conversion of three catalysts Ni/LZ, Ni/L and Ni/Z are provided in Figure 4.1. As reported in previous studies [8, 9, 15, 17, 18], the highest CO_2 conversion of 39.1% was achieved at $CO_2/G = 1$ and it exhibits a decreasing trend with increasing CO_2/G ratio. However, the closest CO_2 conversion value of Ni/LZ to thermodynamic limit attained at CO_2/G ratio of 2. Therefore, $CO_2/G = 2$ determined the course of this study and rest of the results were obtained at this particular feed composition. On the other hand, Ni/L showed increasing trend with increasing CO_2/G ratio whereas Ni/Z showed more complicated response to the increasing CO_2/G ratio which increased up to CO_2/G ratio of 2 and than decreased with increasing ratio. Siew *et al.* [10, 11] have conducted two different studies that support this behavior. According to these studies, increasing the CO_2/G ratio from 0 to 1.68 increases CO_2 conversion and from that point, conversion starts to decrease which clarifies the response of Ni/Z to elevated CO_2/G.

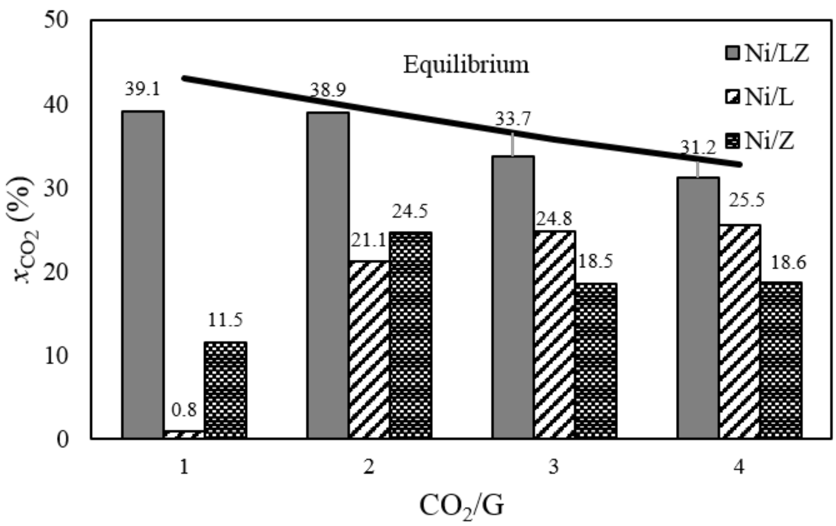

Figure 4.1. Thermodynamic and experimental CO_2 conversions with respect to CO_2/G ratios at 750°C.

The relationship between CO_2/G and CO_2 conversion may also be attributed to CH_4 dry reforming. Lower concentration of CO_2 (means lower CO_2/G ratio) results in insufficient dry reforming of CH_4 which may explain excess CH_4 in product stream and lower CO_2 conversion. Moreover, higher CO_2/G ratio boosts RWGS reaction which produces H_2O. This water may be used in steam reforming of hydrocarbons particularly of CH_4.

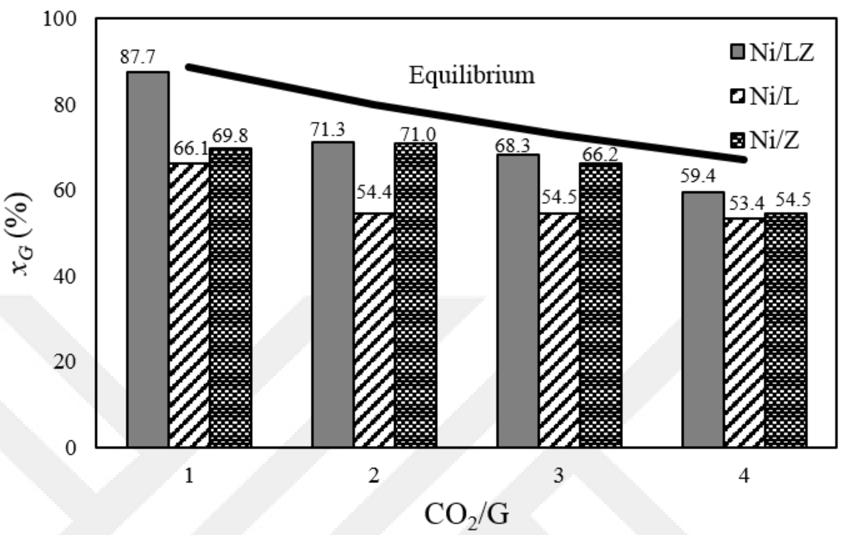

Figure 4.2. Thermodynamic and experimental glycerol conversions with respect to CO_2/G ratios at 750°C.

Figure 4.2 shows glycerol conversion of three catalysts Ni/LZ, Ni/L and Ni/Z together with thermodynamic conversion limits versus CO_2/G ratio. Glycerol conversion of all catalysts tended to increase with decreasing CO_2/G due to RWGS reaction. Higher CO_2 amount in reactant stream diverts reaction to the H_2O side. Although H_2O amount increased with increasing CO_2/G ratio, H_2O was not taken into account while calculating glycerol conversion to gaseous product as explained in Section 3.4.4. The difference between thermodynamic limits and experimental results can be ascribed to dry reforming of methane as explained previously. At CO_2/G ratio of 1, Ni/LZ achieved the highest conversion which is 87.7%.

Tables 4.3 and 4.4 shows product yields and selectivities of three catalysts (Ni/LZ, Ni/L and Ni/Z), respectively. According to both, experiment and thermodynamic analysis, H_2 and CO yields exhibited opposite behavior. While H_2 yield increased with decreasing CO_2/G (shown in Figure 4.3), CO yield demonstrated reverse action (shown in Figure 4.4) which was again caused by RWGS reaction. Increasing CO_2/G

Table 4.3. Product yields at four CO_2/G ratios at 750°C.

	CO_2/G	Y_{H_2}	Y_{CO}	Y_{CH_4}	$Y_{C_2H_4}$	$Y_{C_2H_6}$	H_2/CO	x_{CO_2}(%)	x_G(%)
Ni/LZ	**1**	3.51	2.53	0.00	0.00	0.00	1.39	39.06	87.65
	2	2.85	2.59	0.00	0.00	0.00	1.10	38.95	71.28
	3	2.73	2.98	0.00	0.00	0.00	0.92	33.70	68.31
	4	2.37	3.06	0.00	0.00	0.00	0.78	31.21	59.36
Ni/L	**1**	2.21	2.64	0.20	0.00	0.01	0.84	0.84	66.09
	2	1.87	2.76	0.15	0.00	0.01	0.67	21.11	54.39
	3	1.85	2.96	0.16	0.00	0.00	0.62	24.79	54.48
	4	1.87	3.20	0.13	0.00	0.00	0.58	25.51	53.43
Ni/Z	**1**	2.39	2.78	0.19	0.00	0.00	0.86	11.52	69.85
	2	2.80	2.57	0.02	0.00	0.00	1.09	24.52	70.97
	3	2.35	2.46	0.14	0.00	0.00	0.96	18.47	66.19
	4	1.98	2.94	0.10	0.00	0.00	0.67	18.64	54.55

Table 4.4. Product selectivities at four CO_2/G ratios at 750°C.

	CO_2/G	S_{H_2}	S_{CO}	S_{CH_4}	$S_{C_2H_4}$	$S_{C_2H_6}$
Ni/LZ	**1**	4.00	2.88	0.00	0.00	0.00
	2	4.00	3.64	0.00	0.00	0.00
	3	4.00	4.36	0.00	0.00	0.00
	4	4.00	5.16	0.00	0.00	0.00
Ni/L	**1**	3.34	4.00	0.31	0.01	0.01
	2	3.43	5.08	0.27	0.00	0.01
	3	3.39	5.44	0.29	0.00	0.01
	4	3.50	5.99	0.24	0.00	0.01
Ni/Z	**1**	3.42	3.98	0.00	0.00	0.01
	2	3.95	3.61	0.00	0.00	0.00
	3	3.55	3.71	0.00	0.00	0.01
	4	3.62	5.38	0.00	0.00	0.01

ratio directs reaction route to CO and H_2O side which results in a decrease in H_2 while an increase in CO amount at the same time. Therefore, by changing CO_2/G ratio, desired syngas composition can be obtained.

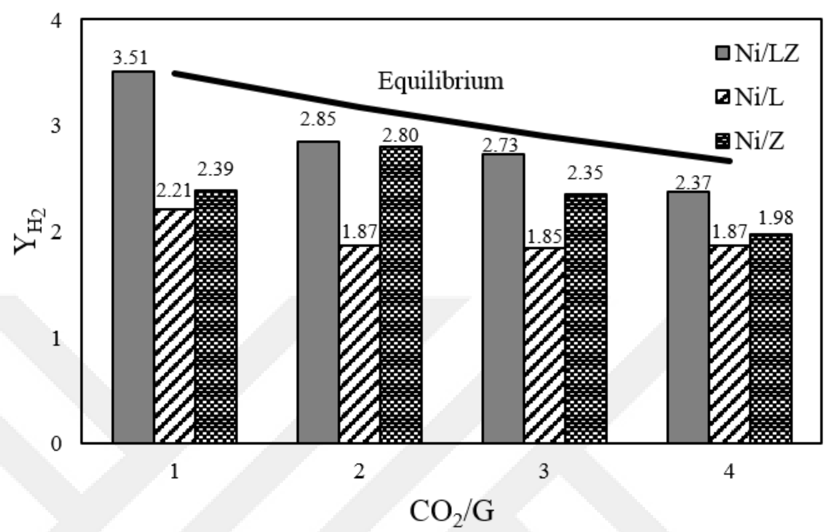

Figure 4.3. Thermodynamic and experimental H_2 yield with respect to CO_2/G ratios at 750°C.

Three major by-products of glycerol dry reforming reaction, which are CH_4, C_2H_4 and C_2H_6 in product stream, are indicators of catalyst deactivation. This is due to the fact that the C_1-C_2 hydrocarbons cannot be consumed due to the reduced catalytic activity towards their steam and dry reforming to syngas. CO_2/G ratio examination of this study showed that Ni/LZ exhibited superior catalytic activity since no CH_4, C_2H_4 and C_2H_6 were produced at any CO_2/G ratio while there was a trace amount of ethane in the product stream of Ni/Z. On the other hand, Ni/L catalyst had both, methane and ethane, in the product stream. This can be interpreted as Ni/Z has better catalytic activity towards methane reforming reactions (steam and dry reforming) while Ni/LZ has capability to catalyze methane, ethane and ethylene reforming reactions in the best manner.

Summing up all ratio examination results, Ni/LZ had better CO_2 and glycerol conversion at all CO_2/G ratios. However, CO_2 conversion was closest to thermodynamic limit at CO_2/G = 2. Moreover, absence of CH_4, C_2H_4 and C_2H_6 in product stream of glycerol dry reforming reaction over Ni/LZ pointed out superior activity of Ni/LZ. It was probably because of the fact that La addition to the Zr support enhanced the number of O_2 vacancies which then pretended as sites that CO_2 can adsorb. Since more CO_2 adsorbed on catalyst surface, activity of the Ni/Z was boosted by La addition [43]. Therefore, all remaining examinations (effect of temperature and residence time and longevity study) were performed at CO_2/G ratio of 2.

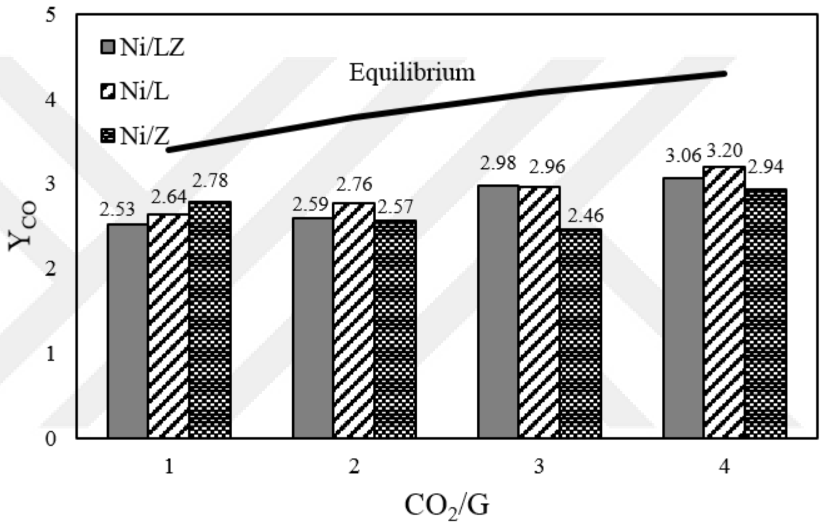

Figure 4.4. Thermodynamic and experimental CO yield with respect to CO_2/G ratios at 750°C.

4.2. Effect of Temperature

Similar to the feed composition, temperature also has strong impact of glycerol and CO_2 conversions as well as product yield and selectivity. As explained in Section 4.1.2, temperature effect investigation and temperature dependent thermodynamic analysis were performed at CO_2/G = 2. For providing further insight into the effects of temperature, thermodynamic analysis performed before activity test and their comparison were reported.

Table 4.5. Thermodynamic product yields at 700 and 750°C.

T(°C)	Y_{H_2}	Y_{CO}	Y_{CO_2}	Y_{CH_4}	Y_{H_2O}	H_2/C	x_{CO_2}(%)	x_G(%)
700	3.16	3.63	1.33	0.05	0.73	0.87	33.88	81.67
750	3.17	3.78	1.22	0.01	0.80	0.84	39.32	79.95

Table 4.6. Thermodynamic product selectivities at 700 and 750°C.

T(°C)	S_{H_2}	S_{CO}	S_{CO_2}	S_{CH_4}	S_{H_2O}
700	3.87	4.44	1.62	0.07	0.90
750	3.97	4.72	1.52	0.02	1.00

4.2.1. Thermodynamic Analysis

Temperature dependent thermodynamic limits were determined by means of CHEMCAD software as done in Section 4.1.1. CO_2/G ratio of the system was kept constant at 2 and two temperatures, 700 and 750°C, were tested. Product yields together with CO_2 and glycerol conversion and product selectivities were tabulated in Table 4.5 and Table 4.6, respectively. The reason why some of the possible products were not included in these tables is that their yield and selectivity values are zero.

Thermodynamic analysis showed that with decreasing temperature, both H_2 and CO yields decreased. However, H_2/CO ratio showed increasing behavior through decreasing temperature since decrease in the CO yield was more significant compared to H_2. In addition, CO_2 conversion tends to increase with temperature increment while glycerol conversion exhibits opposite behavior which increases with decreasing temperature.

4.2.2. Activity Tests

Figure 4.5 shows CO_2 conversion on (Ni/LZ, Ni/L and Ni/Z) together with thermodynamic CO_2 conversion limits at two temperatures. It was seen that the temperature had a positive impact on CO_2 conversion. Ni/LZ achieved 39% conversion which almost reached the thermodynamic limit of 39.32% . Although Ni/L and Ni/Z had relatively lower conversion values compared to Ni/LZ, they exhibited similar behavior against temperature change from 700 to 750°C. Conversion decrease along with decreasing temperature can be attributed to catalyst deactivation due to coke deposition on catalyst surface which tends to be favored at reduced temperatures.

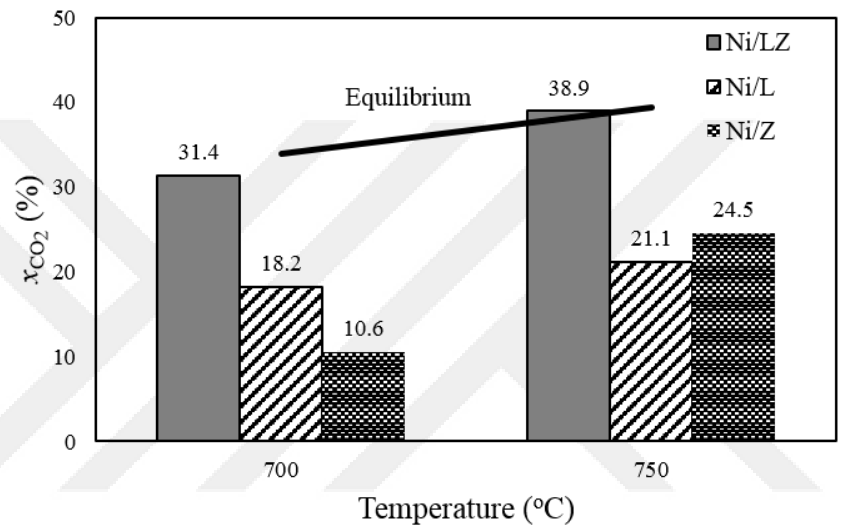

Figure 4.5. Thermodynamic and experimental CO_2 conversion with respect to temperature at CO_2/G=2.

RWGS reaction is moderately endothermic and by increasing the temperature, CO amount increases while H_2 quantity decreases as presented in Table 4.7. Moreover, H_2O amount also increased beside CO quantity and excess amount of H_2O can be used in steam reforming of hydrocarbons (especially C_2H_4 and C_2H_6) which can be attributed to their quantity decrease in product stream with increasing temperature. On the other hand, methane dry reforming reaction can be catalyzed at higher temperatures which clarified the quantity decrease of methane in product stream with elevated temperature.

Glycerol conversion obtained on the current catalysts with respect to temperature is presented in Figure 4.6. Both, thermodynamic and experimental determinations had similar response to temperature change. By increasing temperature from 700 to

Table 4.7. Product yields at 700 and 750°C.

	T(°C)	Y_{H_2}	Y_{CO}	Y_{CH_4}	$Y_{C_2H_4}$	$Y_{C_2H_6}$	H_2/CO	x_{CO_2}(%)	x_G(%)
Ni/LZ	**700**	3.15	2.66	0.00	0.00	0.00	1.18	31.40	78.69
	750	2.85	2.59	0.00	0.00	0.00	1.10	38.95	71.28
Ni/L	**700**	2.08	2.70	0.17	0.00	0.01	0.77	18.18	60.92
	750	1.87	2.76	0.15	0.00	0.01	0.67	21.11	54.39
Ni/Z	**700**	2.04	2.69	0.20	0.01	0.01	0.76	10.59	62.27
	750	2.80	2.57	0.02	0.00	0.00	1.09	24.52	70.97

750°C, glycerol conversion decreased due to domination of the RWGS reaction. As explained before, high temperatures shift direction of RWGS reaction to the H_2O side. However, liquid compounds in products stream are not taken into account when glycerol conversion to gaseous product is obtained. Therefore, glycerol conversion was affected negatively by increasing temperature. As seen in Figure 4.5 and Figure 4.6, Ni/LZ had higher glycerol and CO_2 conversion at two temperatures which is interpreted as superior catalytic activity of Ni/LZ compared to the other two catalysts.

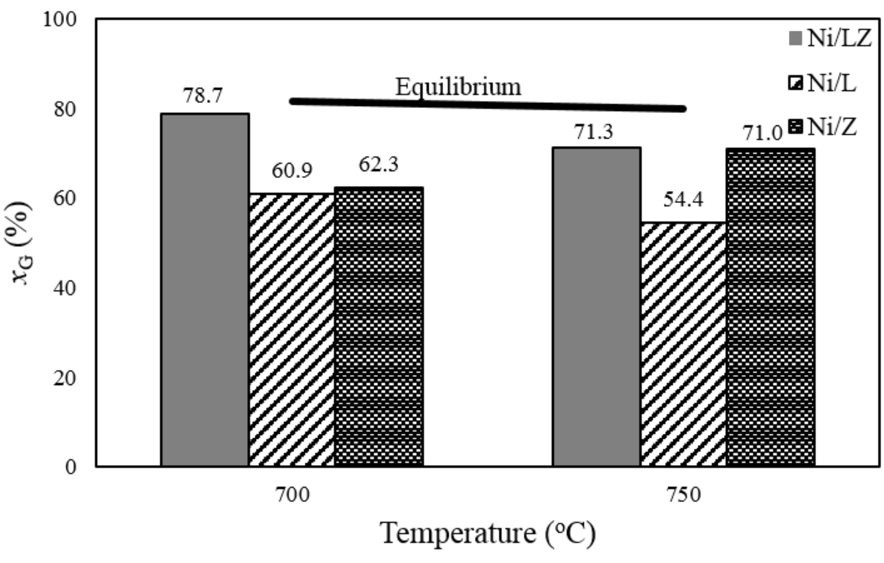

Figure 4.6. Thermodynamic and experimental glycerol conversion with respect to temperature at CO_2/G=2.

In Table 4.7 and Table 4.8, product yield and selectivity of each gaseous compound of the product stream, respectively are presented. By increasing temperature from 700 to 750°C, H_2 and CO yields on Ni/LZ increased. Since increase in H_2 yield

Table 4.8. Product selectivities at 700 and 750°C.

	T(°C)	S_{H_2}	S_{CO}	S_{CH_4}	$S_{C_2H_4}$	$S_{C_2H_6}$
Ni/LZ	**700**	4.00	3.38	0.00	0.00	0.00
	750	4.00	3.64	0.00	0.00	0.00
Ni/L	**700**	3.43	5.08	0.27	0.00	0.01
	750	3.41	4.44	0.27	0.00	0.02
Ni/Z	**700**	3.27	4.32	0.32	0.01	0.02
	750	3.95	3.61	0.02	0.00	0.00

was sharper than CO yield, H_2/CO ratio increased from 1.10 to 1.18 at elevated temperatures.

Figure 4.7 and Figure 4.8 showed H_2 and CO yields along with their thermodynamic yields with respect to temperature. H_2 and CO yields of Ni/LZ which are 2.85 and 3.15, respectively were closest to the pertinent thermodynamic barriers compared to Ni/Z and Ni/L catalysts at both temperatures.

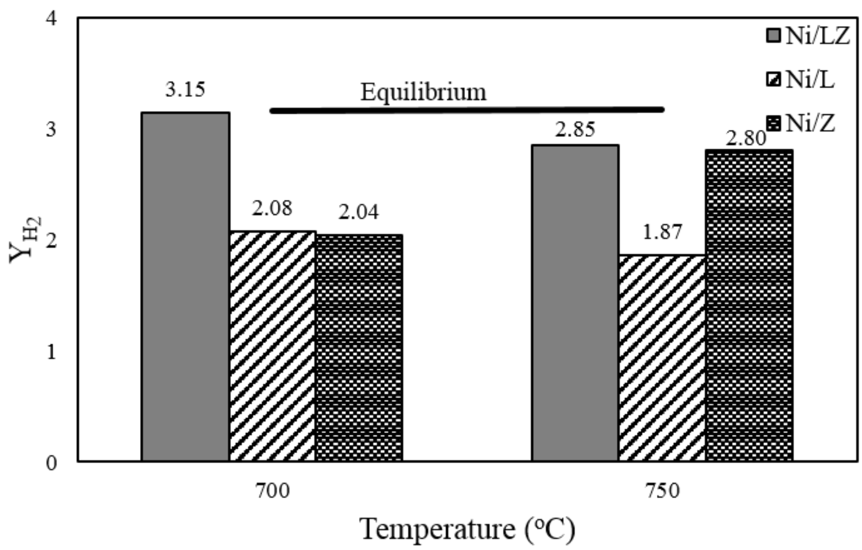

Figure 4.7. Thermodynamic and experimental H_2 yield with respect to temperature at CO_2/G=2.

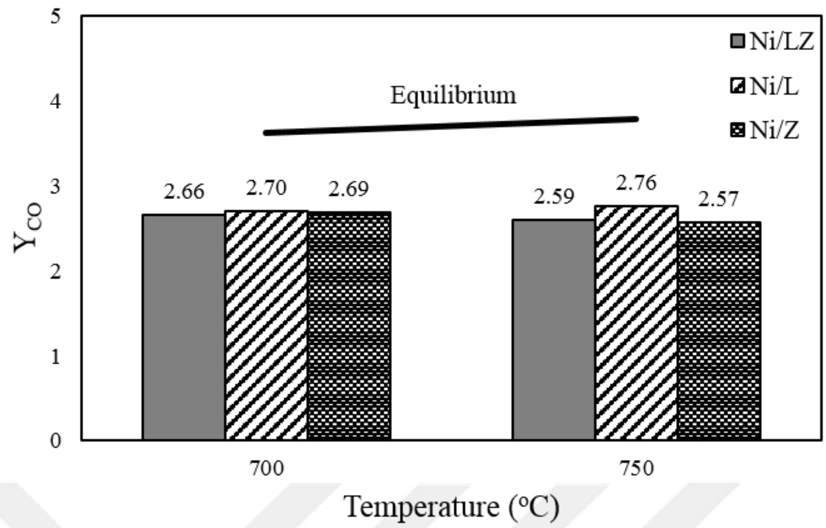

Figure 4.8. Thermodynamic and experimental CO yield with respect to temperature at CO_2/G=2.

The existence of methane, ethane and ethylene in product effluent was interpreted as catalyst deactivation. This was because those hydrocarbons located on active metal side which,thereafter after resulted in deactivation of catalysts. As seen in Table 4.7 and 4.8, product stream of Ni/LZ did not contain any of the C_1-C_2 hydrocarbons at any condition. On the other hand, product effluents of Ni/L and Ni/Z consist of these hydrocarbons with differing compositions depending on reaction conditions. When temperature increases from 700 to 750°C, especially methane selectivity is decreased. The reason of this decrease can possibly be attributed to increased extents of the dry and steam reforming mechanisms.

H_2/CO ratio of 1 is desirable for FTS. It is observed that both Ni/LZ and Ni/Z are capable of delivering syngas ratios of 1.10 and 1.09, respectively at $CO_2/G = 2$ and 750°C. However, comparing these two catalysts according to their CO_2 and glycerol conversions, Ni/LZ is found to be more active than Ni/Z, which means that La addition enhances the activity of Ni/Z.

Bringing all findings together, Ni/LZ achieved 39% CO_2 conversion and 1.10 H_2/CO ratio at 750°C and CO_2/G ratio of 2. Later in this work, residence time examination and stability tests were performed under these these conditions.

4.3. Effect of Residence Time

Residence time has a considerable impact on catalyst activity. In this work, different catalyst amounts were tested to examine the effect of residence time on activity. Figure 4.9 shows CO_2 conversion of Ni/L and Ni/Z with respect to catalyst amount of 20, 50 and 100 mg corresponding to 0.5, 1.25 and 2.5 mg_{cat} min NmL^{-1} residence time, respectively. Residence time investigation was only conducted for Ni/L and Ni/Z not for Ni/LZ since even 20 mg Ni/LZ catalyst achieved 38.9% CO_2 conversion which was very close to the thermodynamic barrier. It is observed that with increasing residence time, CO_2 conversion of both Ni/L and Ni/Z catalysts increases. As seen in Figure 4.10, glycerol conversion of Ni/L and Ni/Z also had a similar incremental trend. Increasing catalyst amount from 20 to 100 mg, glycerol conversion of Ni/L increased from 21.1% to 32.3% while Ni/Z increased from 24.5% to 37.4%.

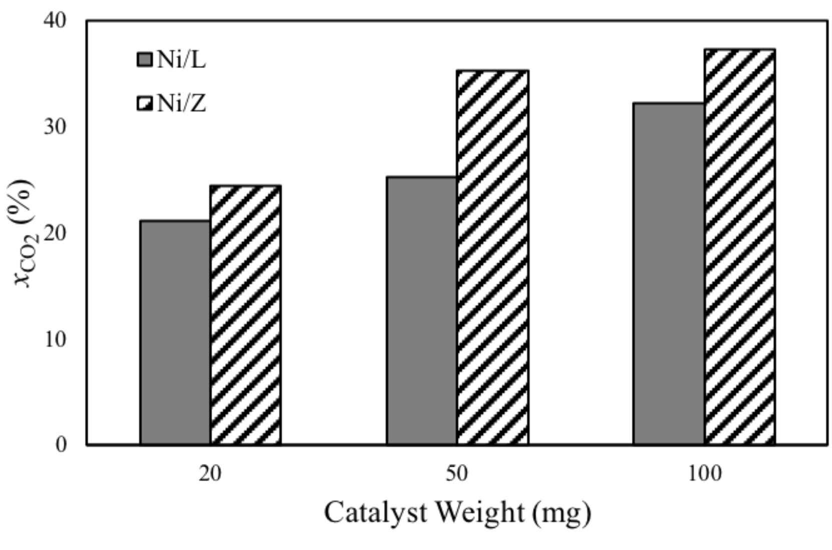

Figure 4.9. CO_2 conversion with respect to catalyst weight at 750°C and CO_2/G = 2.

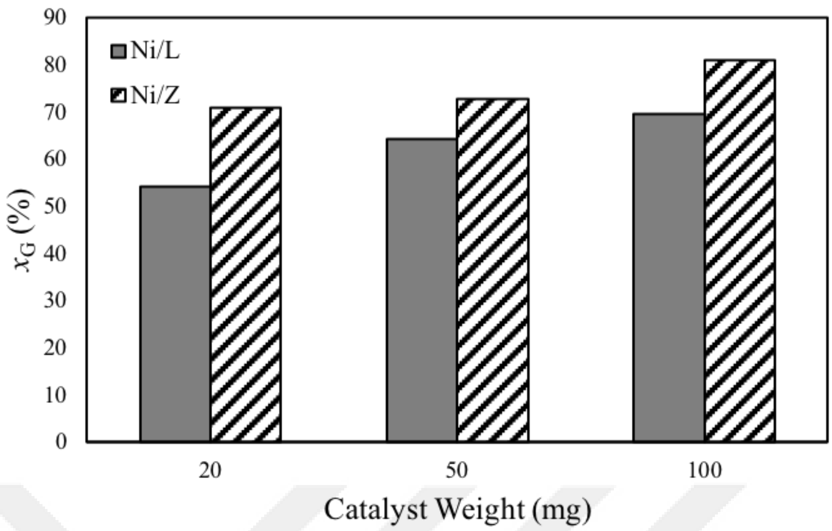

Figure 4.10. Glycerol conversion with respect to catalyst weight at 750°C and CO_2/G=2.

Figure 4.11 compares the three catalysts on the basis of their residence times. Increasing residence time from 0.5 to 3.75 mg_{cat} min NmL^{-1} affected CO_2 conversion positively and this behavior was observed for three catalyst indiscriminately. In addition to CO_2 conversion, glycerol conversion also increased with elevating residence time from 0.5 to 3.75 mg_{cat} min NmL^{-1}. For Ni/LZ, both CO_2 and glycerol conversion which are presented in Figure 4.11 and Figure 4.12, respectively did not change due to superior activity of catalyst which achieved higher conversions even at the lowest catalyst amount. On the other hand, increasing catalyst amount affected CO_2 and glycerol conversions of Ni/L and Ni/Z significantly.

To sum up, while an increase in residence time enhances activity of Ni/L, it boosts activity of Ni/Z to some extent, *i.e.* up to 2.5 mg_{cat} min NmL^{-1}. Further increase in residence time does not make any change on catalytic activity of Ni/Z. Besides, an increase of catalyst amount does not affect activity of Ni/LZ since it has superior activity even over 20 mg catalyst most likely due to the well-dispersed nature of the Ni nanoparticles.

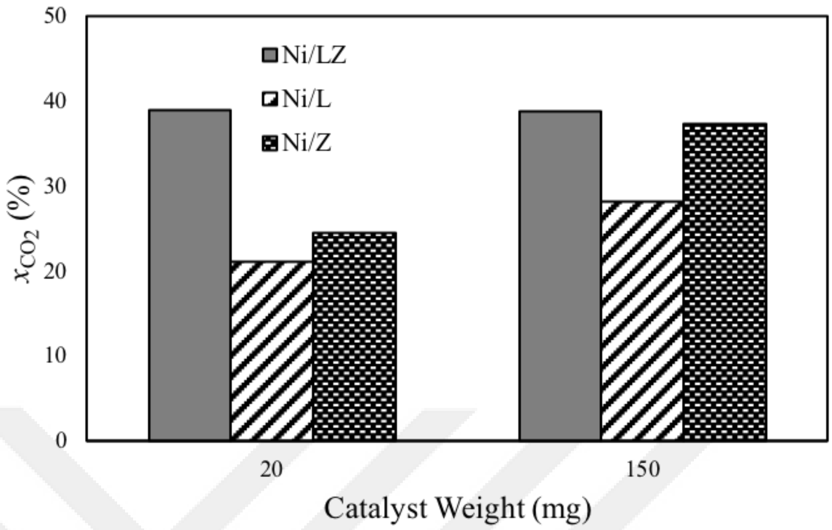

Figure 4.11. CO_2 conversion with respect to catalyst weight at 750°C and CO_2/G= 2.

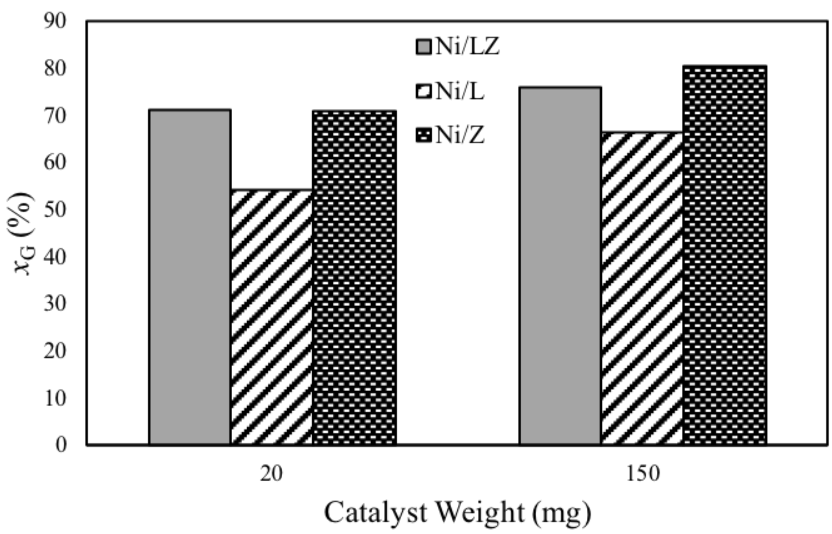

Figure 4.12. Glycerol conversion with respect to catalyst weight at 750°C and CO_2/G=2.

4.4. Stability Test

In order to provide insight into the strength of catalyst over time, stability tests are performed over 150 mg Ni/LZ and Ni/Z catalyst at 750°C and CO_2/G ratio of 2. According to longevity examination of these catalysts, shown in Figure 4.13, Ni/LZ had better stability performance compared to Ni/Z for 72 hours period. At the very beginning of the experiment, it exhibited the highest conversion value of 38.8% CO_2 conversion which was nearly the thermodynamic limit. Over time, its performance did not change considerably and at the end of experiments it achieved 34.7% CO_2 conversion which corresponds to 10.1% activity loss. Interestingly, there is a coherence between literature (9% activity loss [39]) and the stability results found in this study. On the other hand, performance of Ni/Z decreased by time. While it showed notable performance within the first 7 hours (CO_2 conversion was around 36%), activity started to decline incrementally from that point and after 45th hours, the conversion became zero.

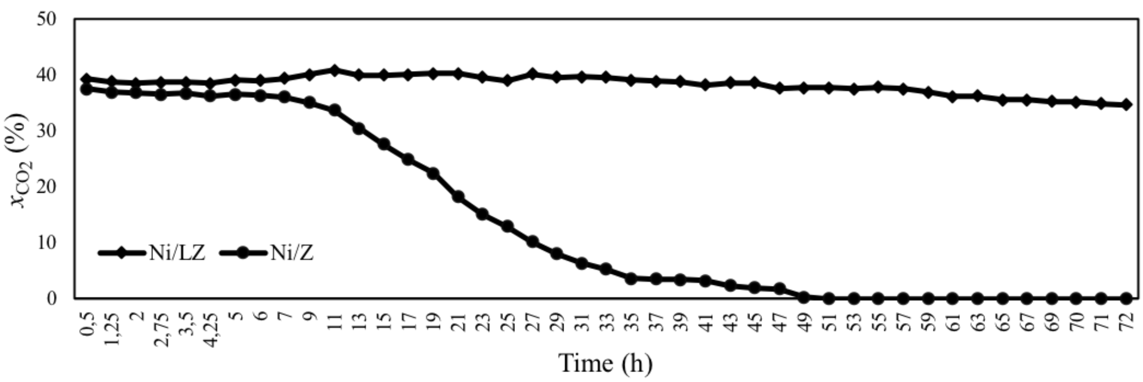

Figure 4.13. CO_2 conversion with respect to 72 h on stream at 750°C and CO_2/G=2.

Possible explanation to Ni/Z deactivation is the coke deposition and sintering and these problematic situation may be eliminated by La_2O_3 addition which suppresses coke deposition by means of improving CO_2 conversion at the basic sites which shift Boudouard reaction to CO side [39]. Moreover, La_2O_3 doping may facilitate stabilization of the catalyst which results in greater performance at time on stream experiments [45, 47].

Table 4.9. Product yields of stability test with respect to time.

	t(h)	Y_{H_2}	Y_{CO}	Y_{CH_4}	$Y_{C_2H_4}$	$Y_{C_2H_6}$	H_2/CO	x_{CO_2}(%)	x_G(%)
Ni/LZ	**2**	2.88	2.94	0.00	0.00	0.00	0.98	38.56	71.96
	5	3.07	3.04	0.00	0.00	0.00	1.01	39.06	76.64
	15	3.00	3.07	0.00	0.00	0.00	098	39.97	74.99
	25	2.92	3.05	0.00	0.00	0.00	0.96	38.99	73.11
	35	3.00	3.11	0.00	0.00	0.00	0.97	39.14	75.12
	45	2.93	3.08	0.00	0.00	0.00	0.95	38.60	73.31
	61	3.06	3.20	0.00	0.00	0.00	0.95	36.21	76.50
	72	2.95	3.16	0.00	0.00	0.00	0.93	34.68	73.64
Ni/Z	**2**	2.92	2.99	0.00	0.00	0.00	0.97	36.85	73.06
	5	2.91	3.02	0.00	0.00	0.00	0.96	36.55	72.73
	15	2.57	2.96	0.02	0.01	0.01	0.87	27.63	66.49
	25	1.92	2.81	0.05	0.03	0.01	0.68	12.99	52.43
	35	1.40	2.84	0.07	0.05	0.01	0.49	3.64	41.71
	45	1.12	2.82	0.07	0.06	0.01	0.37	1.76	35.16

Table 4.10. Product selectivities of stability test with respect to time.

	t(h)	S_{H_2}	S_{CO}	S_{CH_4}	$S_{C_2H_4}$	$S_{C_2H_6}$
Ni/LZ	**2**	4.00	4.08	0.00	0.00	0.00
	5	4.00	3.97	0.00	0.00	0.00
	15	4.00	4.10	0.00	0.00	0.00
	25	4.00	4.17	0.00	0.00	0.00
	35	4.00	4.00	0.00	0.00	0.00
	45	4.00	4.20	0.00	0.00	0.00
	61	4.00	4.19	0.00	0.00	0.00
	72	4.00	4.29	0.00	0.00	0.00
Ni/Z	**2**	4.00	4.09	0.00	0.00	0.00
	5	4.00	4.15	0.00	0.00	0.00
	15	3.87	4.45	0.02	0.02	0.01
	25	3.66	5.37	0.09	0.07	0.01
	35	3.36	6.82	0.16	0.13	0.02
	45	3.18	8.03	0.20	0.18	0.03

5. CONCLUSION

5.1. Conclusion

Glycerol dry reforming over Ni/La_2O_3-ZrO_2, Ni/La_2O_3 and Ni/ZrO_2 catalysts was investigated in this study. The effects of three parameters which are CO_2/G ratio, temperature and residence time on glycerol and CO_2 conversions and product distribution were explored. Moreover, stability tests were performed to observe stability performance of the catalysts. According to the obtained results, the following key conclusions were obtained:

- Decreasing CO_2/G ratio had positive impact on both CO_2 and glycerol conversion of Ni/La_2O_3-ZrO_2.
- While H_2 yield was not affected by CO_2/G ratio changes, CO yield increased with increasing CO_2/G ratio for Ni/La_2O_3-ZrO_2.
- Ni/La_2O_3-ZrO_2 achieved the highest CO_2 conversion at CO_2/G = 2, at which the catalyst functioned very close to the pertinent thermodynamic limits.
- It was observed that the temperature had a positive effect on CO_2 conversion while it had reducing influence on glycerol conversion.
- 750°C was determined to be default temperature to obtain optimum CO_2 conversion.
- At 750°C and CO_2/G = 2, Ni/La_2O_3-ZrO_2 achieved 38.3% CO_2 conversion which was close to its thermodynamic limit and followed by Ni/ZrO_2 with 24.5%.
- Increasing residence time from 0.5 to 2.5 mg_{cat} min NmL^{-1} boosted both glycerol and CO_2 conversions for Ni/La_2O_3 and Ni/ZrO_2.
- While increasing catalyst amount 20 to 150 mg (corresponding to increasing residence time from 0.5 to 3.75 mg_{cat} min NmL^{-1}) improved CO_2 conversion of Ni/La_2O_3 and Ni/ZrO_2, it did not affect Ni/La_2O_3-ZrO_2 since it reached thermodynamic limit even on 20 mg catalysts.
- Increasing catalyst amount from 20 to 100 mg enhanced CO_2 conversion on Ni/ZrO_2 from 24.5% to 37.4%, and on Ni/La_2O_3 from 21.1% to 32.3%.

- Ni/La_2O_3-ZrO_2 showed superior stability performance which had 10.1% activity loss over 72 hours period.
- Ni/ZrO_2 exhibited good stability performance for the first 7 hours period, but its activity decreased incrementally and after 46 hours reached zero.

5.2. Recomendations

The following activities can be carried out to improve the contents of the present study:

- Different Ni loadings can be tested to see the effects on catalytic activity and stability performance.
- Beside different Ni loadings, different support compositions can also be tested by changing the relative amounts of lanthana and zirconia. Such a study will provide further insight into the individual and interactive roles of both oxides.
- Residence time investigation can be extended and optimum catalyst amount for glycerol dry reforming can be determined.
- Catalyst characterization studies should be carried out comparatively on fresh and spent catalysts to provide insight into molecular level understanding of the activity and stability features. These studies are ongoing, but not concluded yet within the time of the preparing the current thesis.
- Stability test can also be performed over Ni/La_2O_3 and comparison to Ni/ZrO_2 and Ni/La_2O_3-ZrO_2 can be done to better understand the effect of La addition. This stability test was planned and will be carried out in the near future.

REFERENCES

1. Administration, U. E. I., *Montly Energy Review, Table1.3 and 10.1*, 2019, https://www.eia.gov/energyexplained/?page=renewable_home, accessed in July 2019.

2. Stelmachowski, M., "Utilization of glycerol, a by-product of the transestrification process of vegetable oils: a review", *Ecological Chemistry and Engineering. S*, Vol. 18, No. 1, pp. 9–30, 2011.

3. Bac Bilgi, S., *A Parametric study on catalyst development for glycerol dry reforming*, Master's Thesis, Boğaziçi University, Turkey, 2018.

4. Bulutoglu, P. S., *Parametric investigation of catalytic dry reforming of glycerol to synthesis gas*, Master's Thesis, Boğaziçi University, Turkey, 2017.

5. Karakaya, M., *Experimental and quantitative analysis of multiphase catalytic reactions under microfluidic conditions and geometries*, Ph.D. Thesis, Bogazici University, Turkey, 2014.

6. National Center for Biotechnology Information, N., *PubChem Database, Glycerol, CID=753*, https://pubchem.ncbi.nlm.nih.gov/compound/Glycerol, accessed in July 2019.

7. Lee, H. C., K. W. Siew, J. Gimbun and C. K. Cheng, "Application of Cement Clinker as Ni-Catalyst Support for Glycerol Dry Reforming", *Bulletin of Chemical Reaction Engineering & Catalysis*, Vol. 8, No. 2, p. 137, 2013.

8. Lee, H. C., K. W. Siew, M. R. Khan, S. Y. Chin, J. Gimbun and C. K. Cheng, "Catalytic performance of cement clinker supported nickel catalyst in glycerol dry reforming", *Journal of Energy Chemistry*, Vol. 23, No. 5, pp. 645–656, 2014, http://dx.doi.org/10.1016/S2095-4956(14)60196-0.

9. Lee, H. C., K. W. Siew, J. Gimbun and C. K. Cheng, "Synthesis and characterisation of cement clinker-supported nickel catalyst for glycerol dry reforming", *Chemical Engineering Journal*, Vol. 255, pp. 245–256, 2014, `http://dx.doi.org/10.1016/j.cej.2014.06.044`.

10. Siew, K. W., H. C. Lee, J. Gimbun and C. K. Cheng, "Characterization of La-promoted Ni/Al2O3 catalysts for hydrogen production from glycerol dry reforming", *Journal of Energy Chemistry*, Vol. 23, No. 1, pp. 15–21, 2014, `http://dx.doi.org/10.1016/S2095-4956(14)60112-1`.

11. Siew, K. W., H. C. Lee, J. Gimbun and C. K. Cheng, "Production of CO-rich hydrogen gas from glycerol dry reforming over La-promoted Ni/Al2O3 catalyst", *International Journal of Hydrogen Energy*, Vol. 39, No. 13, pp. 6927–6936, 2014, `http://dx.doi.org/10.1016/j.ijhydene.2014.02.059`.

12. Siew, K. W., H. C. Lee, M. R. Khan, J. Gimbun and C. K. Cheng, "CO2 reforming of glycerol over La-Ni/Al2O3 catalyst: A longevity evaluative study", *Journal of Energy Chemistry*, Vol. 24, No. 3, pp. 366–373, 2015.

13. Siew, K. W., H. C. Lee, J. Gimbun, S. Y. Chin, M. R. Khan, Y. H. Taufiq-Yap and C. K. Cheng, "Syngas production from glycerol-dry(CO2) reforming over La-promoted Ni/Al2O3 catalyst", *Renewable Energy*, Vol. 74, No. 3, pp. 441–447, 2015.

14. Arif, N. N. M., D.-V. N. Vo, M. T. Azizan and S. Z. Abidin, "Carbon dioxide dry reforming of glycerol for hydrogen production using Ni/ZrO2 and Ni/CaO as catalysts", *Bulletin of Chemical Reaction Engineering & Catalysis*, Vol. 11, No. 2, pp. 200–209, 2016.

15. Mohd Arif, N. N., N. Harun, N. M. Yunus, D.-V. N. Vo, M. T. Azizan and S. Zainal Abidin, "Reforming of glycerol for hydrogen production over Ni based catalysts: Effect of support type", *Energy Sources, Part A: Recovery, Utilization, and Environmental Effects*, Vol. 39, No. 7, pp. 657–663, 2017.

16. Arif, N. N. M., S. Z. Abidin, O. U. Osazuwa, D.-V. N. Vo, M. T. Azizan and Y. H. Taufiq-Yap, "Hydrogen production via CO2 dry reforming of glycerol over ReNi/CaO catalysts", *International Journal of Hydrogen Energy*, 2018.

17. Harun, N., J. Gimbun, M. T. Azizan and S. Z. Abidin, "Characterization of Ag-promoted Ni/SiO2 catalysts for syngas production via carbon dioxide (CO2) dry reforming of glycerol", *Bulletin of Chemical Reaction Engineering & Catalysis*, Vol. 11, No. 2, pp. 220–229, 2016.

18. Harun, N., S. Z. Abidin, N. N. M. Arif, N. A. M. Razali, M. T. Azizan *et al.*, "Characterization of Ni catalyst supported on α-Al2O3 and SiO2 for Syngas Production via Dry Reforming of Glycerol", *Malaysian Journal of Catalysis*, Vol. 3, No. 2, 2017.

19. Harun, N., S. Z. Abidin, O. U. Osazuwa, Y. H. Taufiq-Yap and M. T. Azizan, "Hydrogen production from glycerol dry reforming over Ag-promoted Ni/Al 2 O 3", *International Journal of Hydrogen Energy*, pp. 213–225, 2019, https://doi.org/10.1016/j.ijhydene.2018.03.093.

20. Tavanarad, M., F. Meshkani and M. Rezaei, "Production of syngas via glycerol dry reforming on Ni catalysts supported on mesoporous nanocrystalline Al2O3", *Journal of CO2 Utilization*, Vol. 24, pp. 298–305, 2018.

21. Tavanarad, M., F. Meshkani and M. Rezaei, "Synthesis and Application of Noble Metal Nanocatalysts Supported on MgAl 2 O 4 in Glycerol Dry Reforming Reaction", *Catalysis Letters*, Vol. 148, No. 1, pp. 164–172, 2018.

22. Bulutoglu, P. S., Z. Say, S. Bac, E. Ozensoy and A. K. Avci, "Dry reforming of glycerol over Rh-based ceria and zirconia catalysts: New insights on catalyst activity and stability", *Applied Catalysis A: General*, Vol. 564, pp. 157–171, 2018.

23. Wang, W. and Y. Wang, "Dry reforming of ethanol for hydrogen production: Thermodynamic investigation", *International Jour-*

nal of Hydrogen Energy, Vol. 34, No. 13, pp. 5382–5389, 2009, http://dx.doi.org/10.1016/j.ijhydene.2009.04.054.

24. Kale, G. R. and B. D. Kulkarni, "Thermoneutral point analysis of ethanol dry autothermal reforming", *Chemical Engineering Journal*, Vol. 165, No. 3, pp. 864–873, 2010, http://dx.doi.org/10.1016/j.cej.2010.10.033.

25. Kumar, A., R. R. Bhosale, S. S. Malik, A. E. Abusrafa, M. A. H. Saleh, U. K. Ghosh, M. J. Al-Marri, F. A. Almomani, M. M. Khader and I. M. Abu-Reesh, "Thermodynamic investigation of hydrogen enrichment and carbon suppression using chemical additives in ethanol dry reforming", *International Journal of Hydrogen Energy*, Vol. 41, No. 34, pp. 15149–15157, 2016, http://dx.doi.org/10.1016/j.ijhydene.2016.06.157.

26. Bellido, J. D. A., E. Y. Tanabe and E. M. Assaf, "Carbon dioxide reforming of ethanol over Ni/Y2O3-ZrO2 catalysts", *Applied Catalysis B: Environmental*, Vol. 90, No. 3-4, pp. 485–488, 2009.

27. Hu, X. and G. Lu, "Syngas production by CO2 reforming of ethanol over Ni/Al2O3 catalyst", *Catalysis Communications*, Vol. 10, No. 13, pp. 1633–1637, 2009, http://dx.doi.org/10.1016/j.catcom.2009.04.030.

28. Zawadzki, A., J. D. Bellido, A. F. Lucrédio and E. M. Assaf, "Dry reforming of ethanol over supported Ni catalysts prepared by impregnation with methanolic solution", *Fuel Processing Technology*, Vol. 128, pp. 432–440, 2014, http://dx.doi.org/10.1016/j.fuproc.2014.08.006.

29. Bahari, M. B., N. H. H. Phuc, B. Abdullah, F. Alenazey and D. V. N. Vo, "Ethanol dry reforming for syngas production over Ce-promoted Ni/Al2O3 catalyst", *Journal of Environmental Chemical Engineering*, Vol. 4, No. 4, pp. 4830–4838, 2016, http://dx.doi.org/10.1016/j.jece.2016.01.038.

30. Bahari, M. B., B. C. Goo, T. L. Pham, T. J. Siang, H. T. Danh, N. Ainirazali and D.-V. N. Vo, "Hydrogen-rich syngas production from ethanol dry reforming on La-doped Ni/Al2O3 catalysts: effect of promoter loading", *Procedia engineering*, Vol. 148, pp. 654–661, 2016.

31. Bahari, M. B., N. H. H. Phuc, F. Alenazey, K. B. Vu, N. Ainirazali and D. V. N. Vo, "Catalytic performance of La-Ni/Al2O3 catalyst for CO2 reforming of ethanol", *Catalysis Today*, Vol. 291, pp. 67–75, 2017, http://dx.doi.org/10.1016/j.cattod.2017.02.019.

32. Bej, B., S. Bepari, N. C. Pradhan and S. Neogi, "Production of hydrogen by dry reforming of ethanol over alumina supported nano-NiO/SiO2 catalyst", *Catalysis Today*, Vol. 291, pp. 58–66, 2017.

33. Wang, S., Q. Wang, X. Song and J. Chen, "Dry autothermal reforming of glycerol with in situ hydrogen separation via thermodynamic evaluation", *International Journal of Hydrogen Energy*, Vol. 42, No. 2, pp. 838–847, 2017, http://dx.doi.org/10.1016/j.ijhydene.2016.09.103.

34. Wang, X., M. Li, M. Wang, H. Wang, S. Li, S. Wang and X. Ma, "Thermodynamic analysis of glycerol dry reforming for hydrogen and synthesis gas production", *Fuel*, Vol. 88, No. 11, pp. 2148–2153, 2009, http://dx.doi.org/10.1016/j.fuel.2009.01.015.

35. Kale, G. R. and B. D. Kulkarni, "Thermodynamic analysis of dry autothermal reforming of glycerol", *Fuel Processing Technology*, Vol. 91, No. 5, pp. 520–530, 2010, http://dx.doi.org/10.1016/j.fuproc.2009.12.015.

36. Freitas, A. C. and R. Guirardello, "Comparison of several glycerol reforming methods for hydrogen and syngas production using Gibbs energy minimization", *International Journal of Hydrogen Energy*, Vol. 39, No. 31, pp. 17969–17984, 2014.

37. Fernández, Y., A. Arenillas, J. M. Bermúdez and J. A. Menéndez, "Comparative study of conventional and microwave-assisted pyrolysis, steam and dry reforming of glycerol for syngas production, using a carbonaceous catalyst", *Journal of Analytical and Applied Pyrolysis*, Vol. 88, No. 2, pp. 155–159, 2010.

38. Bac, S., Z. Say, Y. Kocak, K. E. Ercan, M. Harfouche, E. Ozensoy and A. K. Avci, "Exceptionally active and stable catalysts for CO2 reforming of glycerol to syngas", *Applied Catalysis B: Environmental*, p. 117808, 2019.

39. Sokolov, S., E. V. Kondratenko, M.-M. Pohl, A. Barkschat and U. Rodemerck, "Stable low-temperature dry reforming of methane over mesoporous La2O3-ZrO2 supported Ni catalyst", *Applied Catalysis B: Environmental*, Vol. 113, pp. 19–30, 2012.

40. Xue, Y.-p., C.-f. Yan, X.-y. Zhao, S.-l. Huang and C.-q. Guo, "Ni/La 2 O 3-ZrO 2 catalyst for hydrogen production from steam reforming of acetic acid as a model compound of bio-oil", *Korean Journal of Chemical Engineering*, Vol. 34, No. 2, pp. 305–313, 2017.

41. Angeli, S. D., L. Turchetti, G. Monteleone and A. A. Lemonidou, "Catalyst development for steam reforming of methane and model biogas at low temperature", *Applied Catalysis B: Environmental*, Vol. 181, pp. 34–46, 2016.

42. Li, X., D. Li, H. Tian, L. Zeng, Z.-J. Zhao and J. Gong, "Dry reforming of methane over Ni/La2O3 nanorod catalysts with stabilized Ni nanoparticles", *Applied Catalysis B: Environmental*, Vol. 202, pp. 683–694, 2017.

43. Goula, M., N. Charisiou, G. Siakavelas, L. Tzounis, I. Tsiaoussis, P. Panagiotopoulou, G. Goula and I. Yentekakis, "Syngas production via the biogas dry reforming reaction over Ni supported on zirconia modified with CeO2 or La2O3 catalysts", *international journal of hydrogen energy*, Vol. 42, No. 19, pp. 13724–13740, 2017.

44. Tao, Q., Z. Wang, B. Jayasundera, C. Guo, Y. Gan, L. Zhang, Z. Lu, H. Tan and C. Yan, “Enhanced catalytic activity of Ni–Mo 2 C/La 2 O 3–ZrO 2 bifunctional catalyst for dry reforming of methane”, *Journal of materials science*, Vol. 53, No. 20, pp. 14559–14572, 2018.

45. Cheng, H., G. Li, H. Zhao, X. Lu, Q. Xu and W. Tao, “Effects of preparation technique and lanthana doping on Ni/La2O3-ZrO2 catalysts for hydrogen production by CO2 reforming of coke oven gas”, *Catalysis Today*, Vol. 318, pp. 23–31, 2018.

46. Simsek, E., M. Karakaya, A. K. Avci *et al.*, “Oxidative steam reforming of methane to synthesis gas in microchannel reactors”, *International Jjournal of Hydrogen Energy*, Vol. 38, No. 2, pp. 870–878, 2013.

47. Rezaei, M., S. Alavi, S. Sahebdelfar, P. Bai, X. Liu and Z.-F. Yan, “CO2 reforming of CH4 over nanocrystalline zirconia-supported nickel catalysts”, *Applied Catalysis B: Environmental*, Vol. 77, No. 3-4, pp. 346–354, 2008.

APPENDIX A: CALIBRATION OF MASS FLOW CONTROLLERS

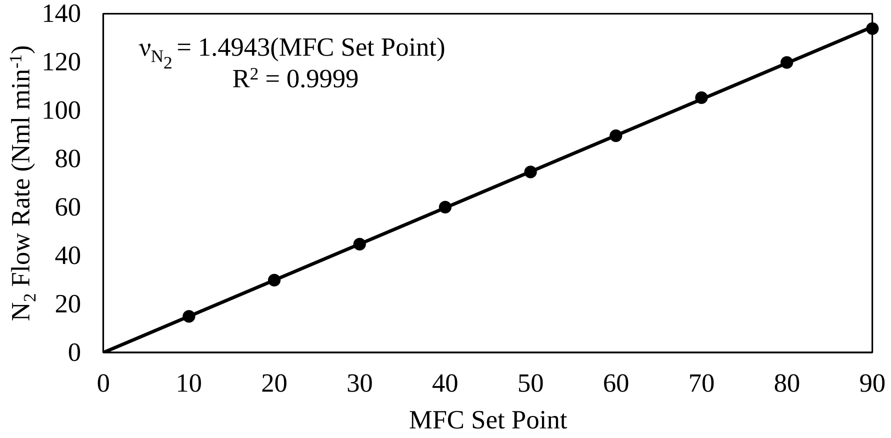

Figure A.1. Calibration curve of MFC for N_2.

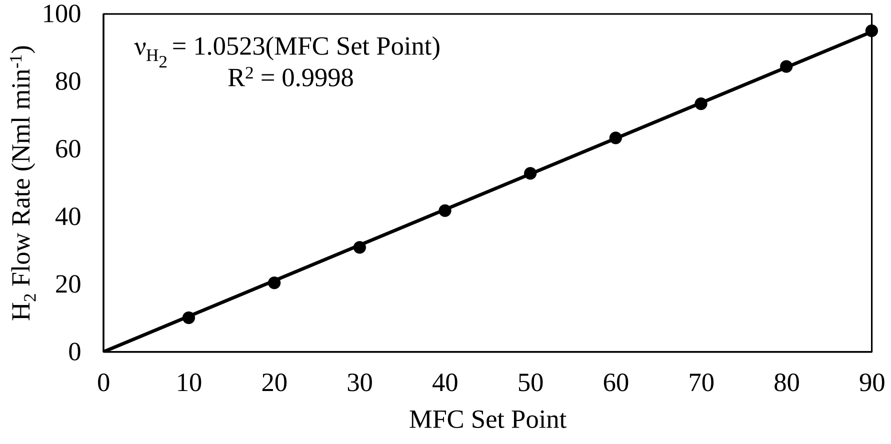

Figure A.2. Calibration curve of MFC for H_2.

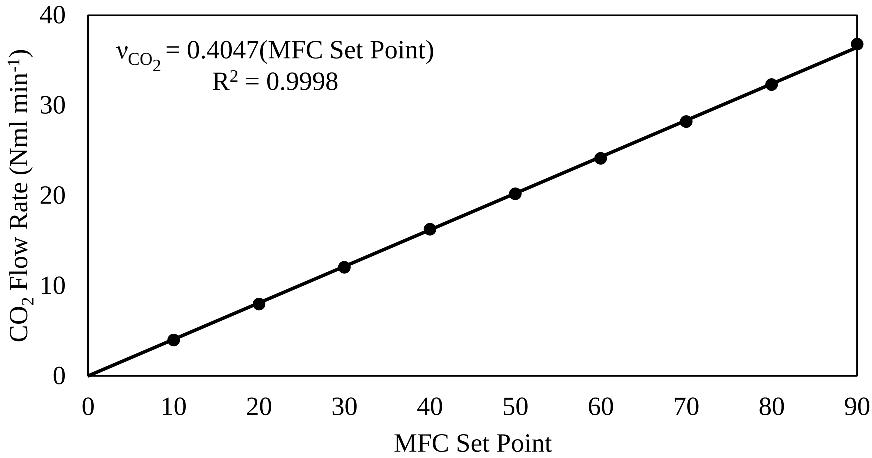

Figure A.3. Calibration curve of MFC for CO_2.

APPENDIX B: CALIBRATION OF GAS CHROMATOGRAPHS

B.1. Calibration Curves for Schimadzu GC-2014

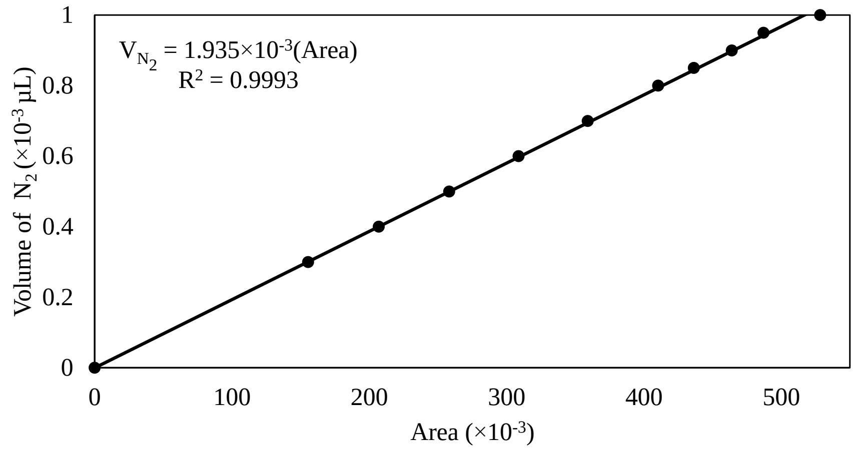

Figure B.1. GC1 calibration curve for N_2.

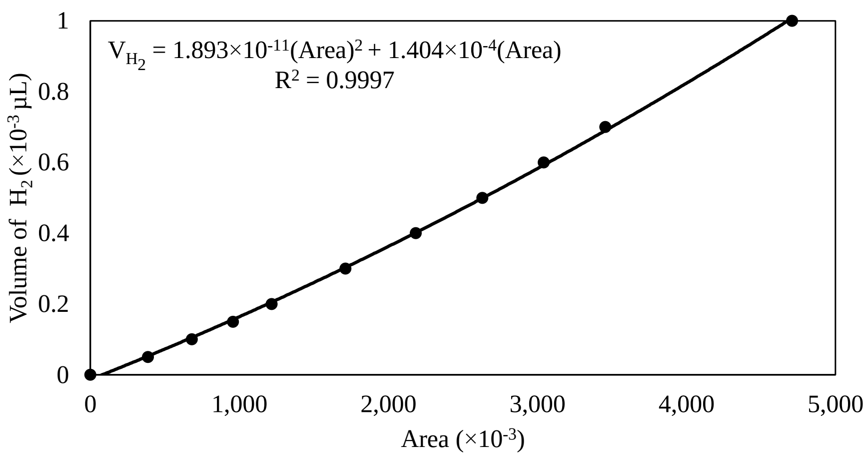

Figure B.2. GC1 calibration curve for H_2.

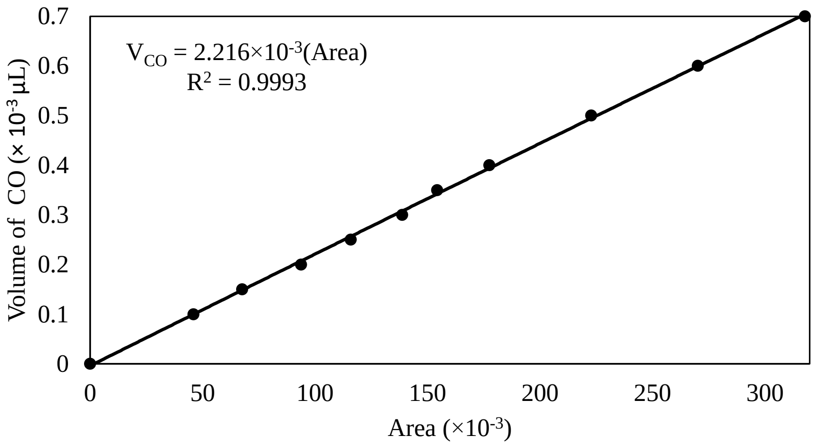

Figure B.3. GC1 calibration curve for CO.

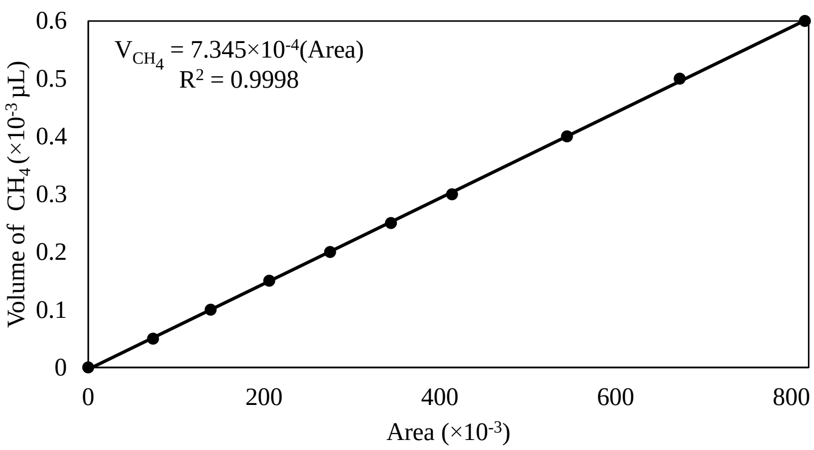

Figure B.4. GC1 calibration curve for CH_4.

B.2. Calibration Curves for Agilent GC-6850

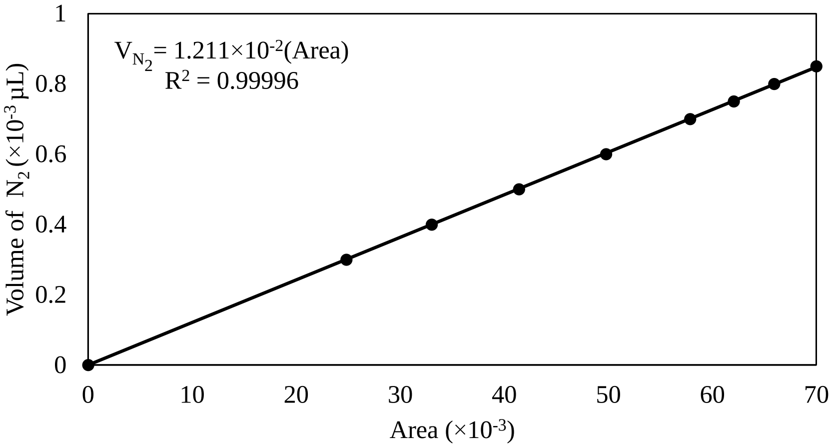

Figure B.5. GC2 calibration curve for N_2.

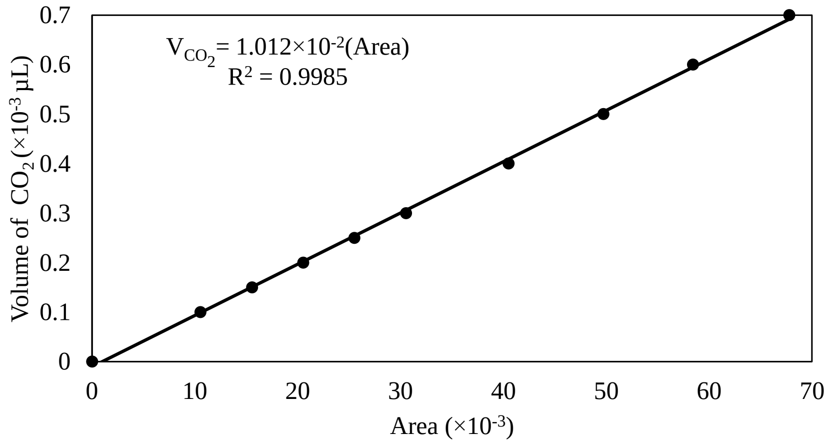

Figure B.6. GC2 calibration curve for CO_2.

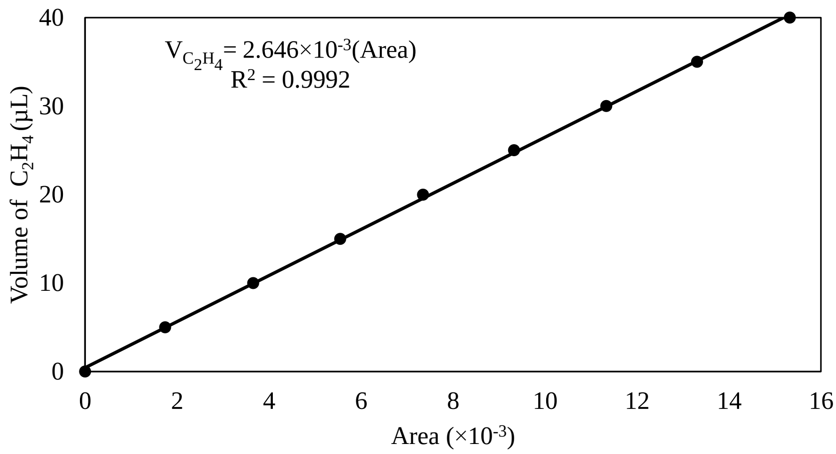

Figure B.7. GC2 calibration curve for C_2H_4.

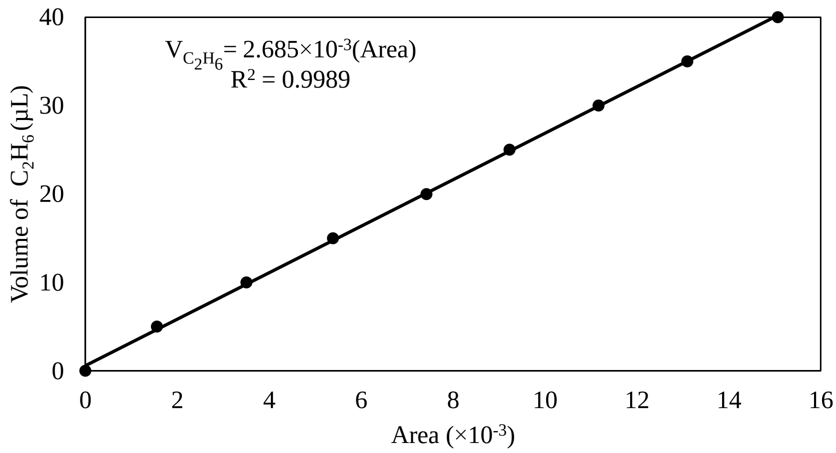

Figure B.8. GC2 calibration curve for C_2H_6.